ACTINIDE RESEARCH QUARTERLY

89 Ac | 90 Th | 91 Pa | 92 U | 93 Np | 94 Pu | 95 Am | 96 Cm | 97 Bk | 98 Cf | 99 Es | 100 Fm | 101 Md | 102 No | 103 Lr

First Quarter 2019

Targeted Radiation Therapy

Seaborg postdocs developing actinide isotopes for cancer treatments

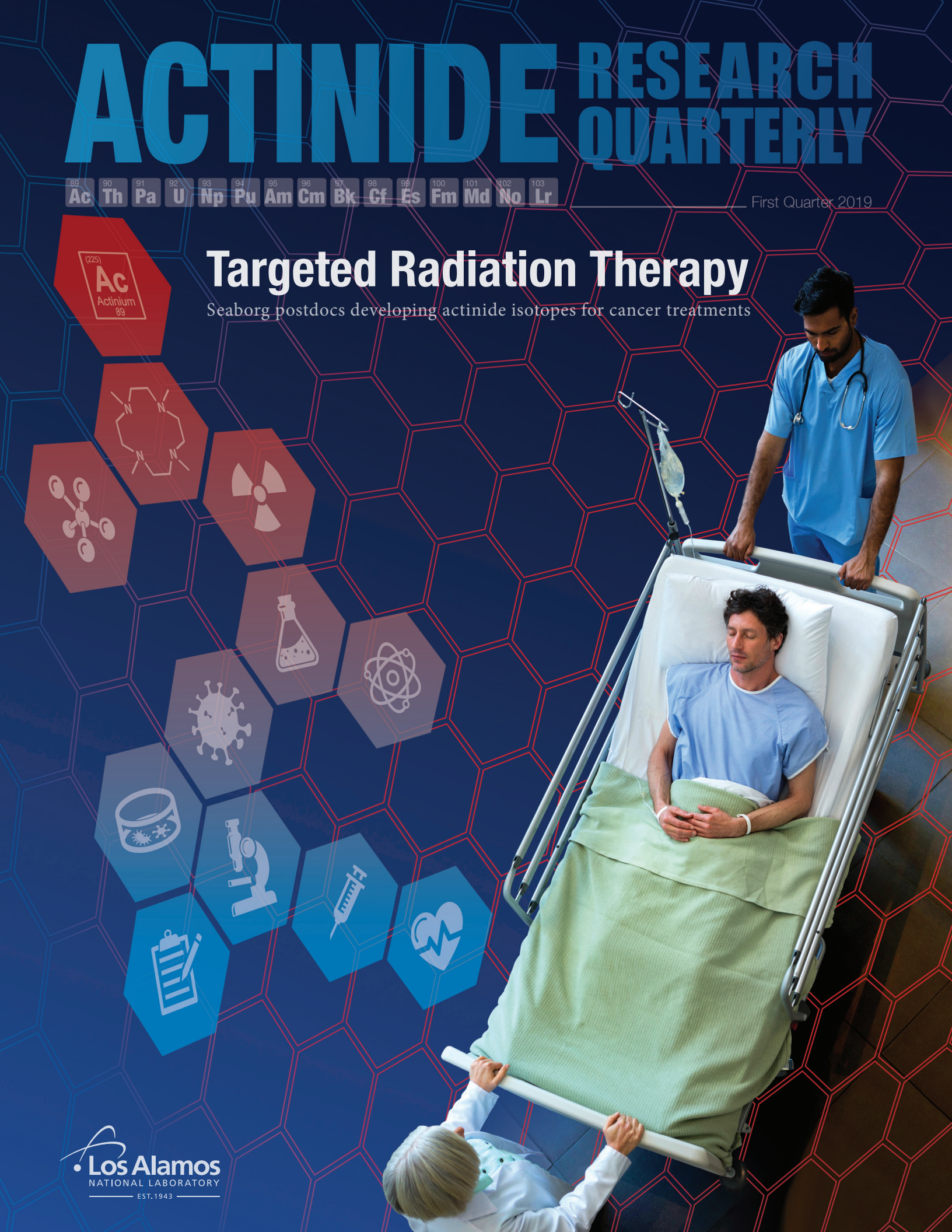

Los Alamos
NATIONAL LABORATORY
EST. 1943

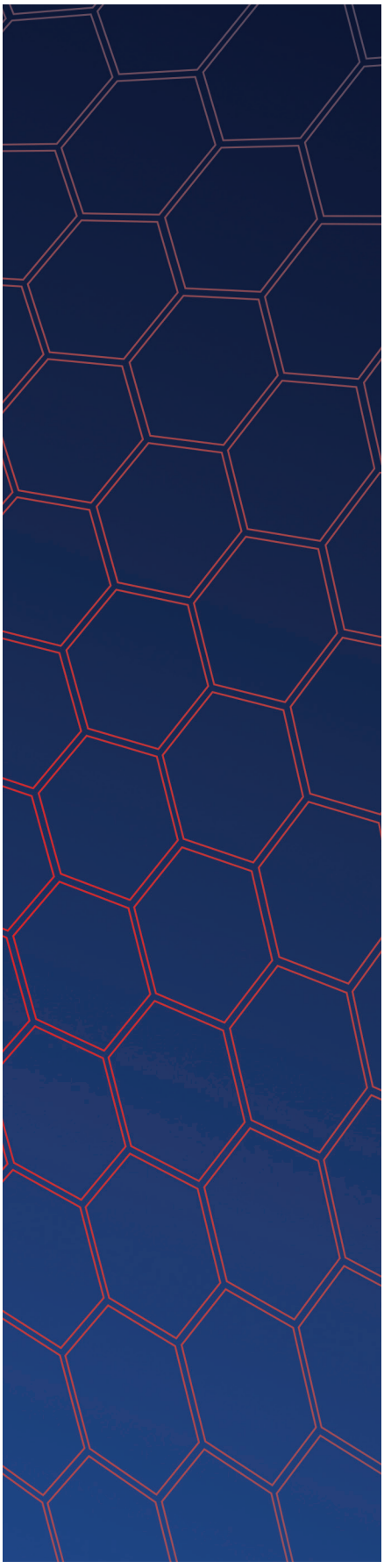

Preface

In this quarter we continue from the previous issue and present research from another seven recent Seaborg postdoctoral fellows, many of whom have continued their work at Los Alamos National Laboratory (LANL) as scientists.

This issue focuses on the chemistry of actinide elements relevant to a wide range of challenges, in particular: the separation of nuclear waste, the application of radionuclides in cancer treatments, and the aging of plutonium in the nation's stockpile.

One of the great challenges in actinide chemistry is understanding and predicting bonding in actinide molecules, which could pave the way for developing nuclear waste separation systems. Su (*p11*) has tackled these problems using advanced computational techniques to understand the nature of chemical bonding in Am^{3+} and Eu^{3+} salts, supported by experimental data, providing direct evidence for the first time to explain behavior originally observed by our institute's namesake Seaborg and his co-workers over 60 years ago. The synthesis of the first Np imido complex—an analog of the well-known neptunyl ion—is described by Brown (*p17*), a milestone achievement that also opens doors for theoretical studies which can improve our understanding of actinide bonding.

The coordination and catalytic chemistry of Th and U has been explored by Browne (*p23*) and Erickson (*p27*), who used similar organometallic platforms to investigate high-nitrogen content molecules as nuclear fuel precursors and hydrogen-generating catalytic cycles, respectively.

The surface of metallic Pu is highly reactive and dynamic, which creates problems when trying to predict how the material will behave, especially in long-term storage (e.g., in the nation's stockpile). Using a new facility at LANL, Hernandez (*p33*) throws some light onto the oxidation and corrosion processes occurring in just the outer 1–2 monolayers of the Pu surface.

The cover highlights work from three more Seaborg fellows on the challenges of developing Ac^{3+} for use in cancer treatments, described on the opposite page.

These articles showcase the problems being addressed by the next generation of scientists, which in particular are pushing boundaries with the more experimentally and theoretically challenging transuranium actinides.

— Owen Summerscales | Editor

In this issue

About the cover: *The short-lived and highly radioactive isotope 225-Ac has gained increasing interest as a weapon in the fight against cancer. Three Seaborg postdocs,* Wilson *(p2),* Stein, and Kerlin *(p7), have developed the basic coordination chemistry—surprisingly absent due to the difficulties of using and obtaining this material—which is essential for designing effective molecules that tether the radionuclide to the cancer-homing antibody.*

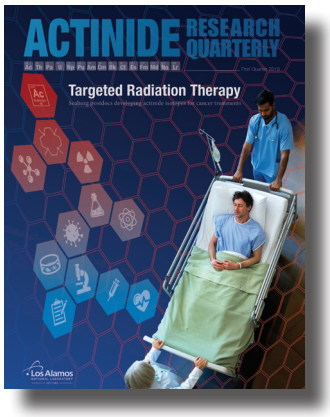

Justin J. Wilson

Justin Wilson was a Seaborg Institute Postdoctoral Research Fellow from August 2013 to June 2015, working under the mentorship of Eva Birnbaum. He is currently an assistant professor in the Department of Chemistry and Chemical Biology at Cornell University. His research interests lie in the design of new radiopharmaceutical agents and the use of inorganic complexes for medical purposes.

Investigating the Chemistry of Actinium, a Therapeutically Relevant Actinide

Actinium (Ac), element 89 on the periodic table, marks the beginning of the actinide series. Unlike its neighbors, its chemistry and chemical properties have scarcely been explored. This knowledge gap is mostly due to the lack of stable or long-lived isotopes of this element—the most abundant isotope of plutonium, ^{239}Pu, for instance, has a half-life of over 24,000 years, whereas the longest-lived isotope of actinium, ^{227}Ac, has a half-life of only 21.77 years. Therefore, capabilities to produce and handle macroscopic quantities of this highly radioactive element are correspondingly very limited. Most of our knowledge of the chemical properties of Ac arises from harrowing studies[1] in the 1950s and 1960s, when researchers engaged in an operation to generate milligram quantities of this element for fundamental studies. Alas, due to the great hazards associated with this work and the scarce availability of Ac, those efforts were largely abandoned, and our understanding of this element has not substantially progressed in the last 50 years. In contrast, the chemistry of the other early actinide elements has been steadily developed throughout the last several decades, with thousands of research articles describing the chemistry of actinides such as plutonium and uranium. The motivations for these research efforts are fairly obvious—these actinides play crucial roles in the nuclear energy cycle and weapons. What uses and applications would suddenly prompt us to be concerned about the 50 year actinium chemistry hiatus?

In contrast to the other actinides, it has become clear within the last two decades that the most important application of Ac lies within the realm of medicine. Although seemingly contradictory to the known radiotoxicity of the actinides, the clinical use of ^{225}Ac is a promising strategy for the treatment of cancer and other diseases, via targeted radionuclide therapy. ^{225}Ac emits a total of four alpha particles throughout its decay chain with a short half-life ($t_{1/2}$ = 9.92 days), which renders it compatible for biological use (see Fig. 1 in subsequent article by Stein and Kerlin, p7). By chemically attaching this isotope via a chelating ligand to an antibody (a large biomolecule that selectively and strongly binds to cell surface receptors of cancer cells), the otherwise damaging alpha particles can be strategically harnessed to destroy malignant tumors (Fig. 1). Preclinical trials of ^{225}Ac-antibody constructs have demonstrated the therapeutic utility of this isotope and general strategy. Highly selective antibodies are well developed, and efforts for large-scale production of ^{225}Ac are also underway. An open question remains, however, regarding the most effective way to chemically attach the Ac ion to the cancer cell-targeting antibody. Displacement of Ac prior to its arrival at the target site will lead to toxic side-effects arising from unselective damage of healthy tissue from its alpha particles. The lack of progress in Ac chemistry has hindered the development of an appropriate chelating agent. A better appreciation and understanding of this element's chemical properties will facilitate new ligand design, enabling the development of safer Ac-based radiopharmaceuticals.

1 On a per mass basis, ^{227}Ac is 2.2×10^{13} times more radioactive than ^{238}U!

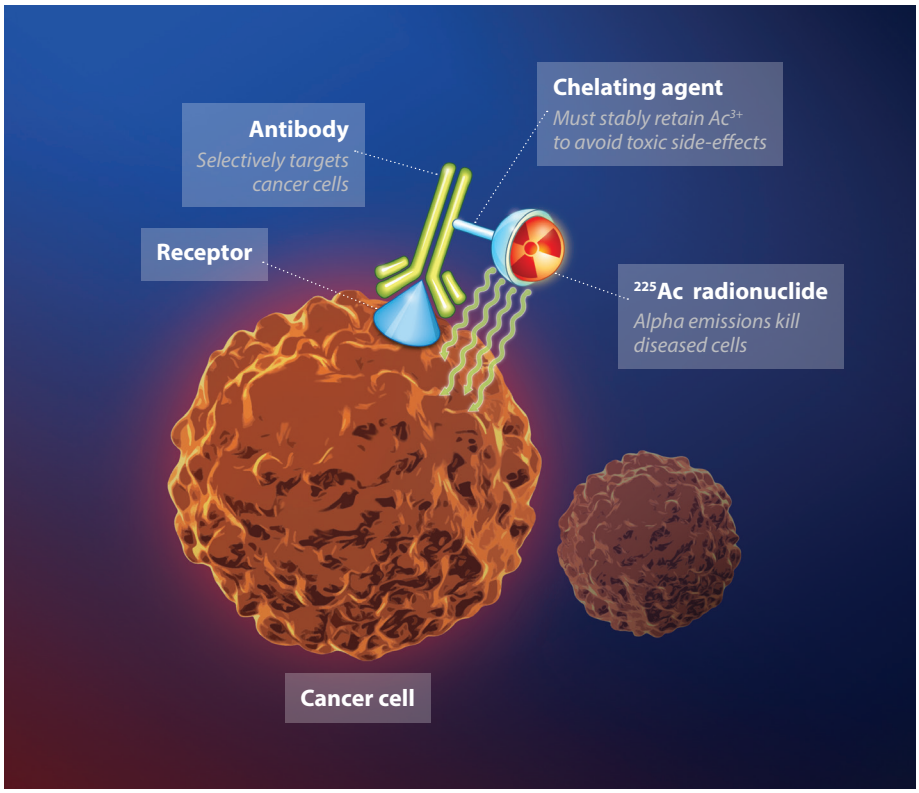

Figure 1. Illustration of the general strategy for using ^{225}Ac in targeted radiotherapy. A biomolecule is used to direct ^{225}Ac to diseased tissue where its alpha particle emissions can kill cells. A weakness in this construct lies in the choice of chelating agent, none of which are well established for Ac^{3+}. By understanding the fundamental chemical properties of this rare ion, optimal chelating agents can be designed and utilized for the development of safer and more effective ^{225}Ac-based radiopharmaceutical agents.

Ac^{3+} chemical properties

Several of the fundamental chemical properties of Ac are known. Only the +3 oxidation state, which has a closed-shell radon electron configuration, is stable in aqueous solution. As a result, the Ac^{3+} ion is diamagnetic with no valence electrons in the 6d or 5f orbitals, rendering this ion spectroscopically silent. A unique property of the Ac^{3+} ion is its large six-coordinate ionic radius of 1.13 Å; Ac^{3+} is the largest trivalent ion in the periodic table. The absolute chemical hardness of an ion, another fundamental property, is a measure of its polarizability. Metal-ligand interactions are dictated by the hard-soft acid-base (HSAB) principle, whereby "hard" ions interact most strongly with "hard" ligands and vice versa. This principle, therefore, dictates the choice of preferred donor atom for a given metal ion. Using density functional theory (DFT) calculations, we computed the chemical hardness of Ac^{3+} to be 14.5 eV. This value classifies Ac^{3+} as a moderately hard ion. Taken together, these data show that Ac^{3+} is the largest +3 ion in the periodic table with a stable noble gas electron configuration and indicate a preference for hard donor atoms.

Ligation studies

With this knowledge in hand, we began our investigation into Ac chemistry by evaluating the relative binding affinity of this ion with the nitrogen-rich macrocycles shown in Fig. 2 (nitrogen being classified as a moderately hard donor atom). The nature of each pendant N-heterocycle varies slightly with regard to chemical hardness. We reasoned that differences in binding affinity might shed light on an optimal value of ligand chemical hardness for forming stable bonds with the Ac ion.

Attempts to radiolabel these ligands with short-lived ^{225}Ac, however, led to an unexpected result. Under all conditions screened, Ac^{3+} did not coordinate to the macrocyclic ligands. Instead, the third daughter isotope of ^{225}Ac, ^{213}Bi, was incorporated rapidly and selectively (see Fig. 1 on p7). This result highlights the

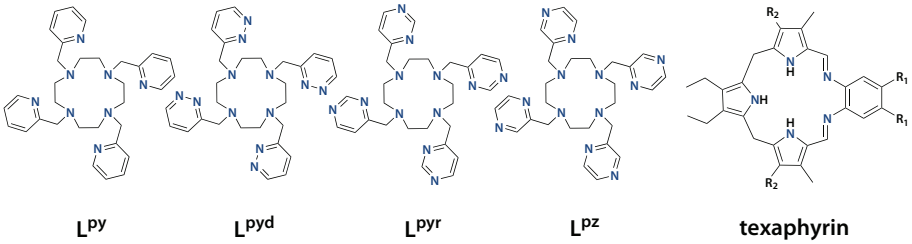

Figure 2. Structures of nitrogen-rich ligands tested for ^{225}Ac labeling. Our studies did not show any radiolabeling with ^{225}Ac, but instead revealed selective labeling of the ^{213}Bi daughter isotope, indicating a poor nitrogen donor atom affinity of Ac^{3+}.

surprisingly low nitrogen atom affinity of the Ac^{3+} ion. Indeed, estimation of the binding constant (K) of Ac^{3+} for a quintessential nitrogen donor ligand, NH_3, gives a relatively small value of log$K$ = 0.8. The higher corresponding value for Bi^{3+} (log$K$ = 5.1) explains the observed selectivity. Additionally, preliminary work utilizing the expanded porphyrin-like macrocycle, texaphyrin (Fig. 2), again demonstrated selective labeling of ^{213}Bi over ^{225}Ac. From these studies, it is clear that an ideal chelating agent for Ac^{3+} should bear some oxygen atom donors (which are less polarizable than nitrogen atoms), or other chemically hard donors, rather than nitrogen donors.

Fluorescence spectroscopy

Additional efforts to understand the chemical properties of Ac^{3+} employed the long-lived isotope, ^{227}Ac ($t_{1/2}$ = 21.77 years). For this research, we were able to utilize a supply of 10 mCi of ^{227}Ac, which corresponds to only 0.61 μmol, or 140 μg, of Ac. The small quantities available, and the challenges associated with handling this highly radioactive element, necessitate a method of chemical analysis that is highly sensitive to low concentrations. We reasoned that fluorescence spectroscopy, a technique that can be commonly used for the detection of sub-micromolar concentrations of analyte, would be an effective method for probing Ac^{3+} chemistry. Because Ac^{3+} is spectroscopically silent, an organic fluorophore with a metal ion-binding unit is needed to relay information. Furthermore, to extract useful data regarding the Ac^{3+} ion, a fluorescent sensor that responds in a metal ion-dependent manner, rather than a simple "on-off" response, is necessary.

These efforts led to the design and synthesis of a new ligand, Ds-DOTAM (Fig. 3). This ligand bears a macrocyclic metal ion-binding unit and a fluorescent dansyl (Ds) group. The hard oxygen atom of the sulfone group of dansyl can interact favorably with similarly hard metal ions, perturbing its photophysical properties. Indeed, addition of the non-radioactive lanthanide $4f^0$ ion La^{3+} (six-coordinate ionic radius 1.03 Å vs. 1.13 Å for Ac^{3+}) to Ds-DOTAM led to a red shift in the absorbance maximum of the ligand (i.e., an increase in wavelength and quenching of the dansyl emission; see Fig. 3). DFT calculations indicate that this red shift arises from a stabilization of the lowest-unoccupied molecular orbital (LUMO), primarily due to an electrostatic interaction of the M^{3+} ion with the dansyl sulfone group. The addition of $Ac(NO_3)_3$ showed similar spectroscopic changes. The UV-vis. absorbance spectrum is, however, partially obscured by the presence of a large excess of NO_3^- ion, which absorbs at 290 nm and is carried over from radiochemical separation procedures. This data indicates that Ac^{3+} and La^{3+} interact with Ds-DOTAM in a similar manner. Nonetheless, strategies to purify the Ac^{3+} ion from excess NO_3^- ions remain an important goal for obtaining high quality spectra.

X-ray absorption spectroscopy

Although the fluorescence spectroscopy results revealed that both La^{3+} and Ac^{3+} interact with Ds-DOTAM, the precise nature of that interaction will certainly

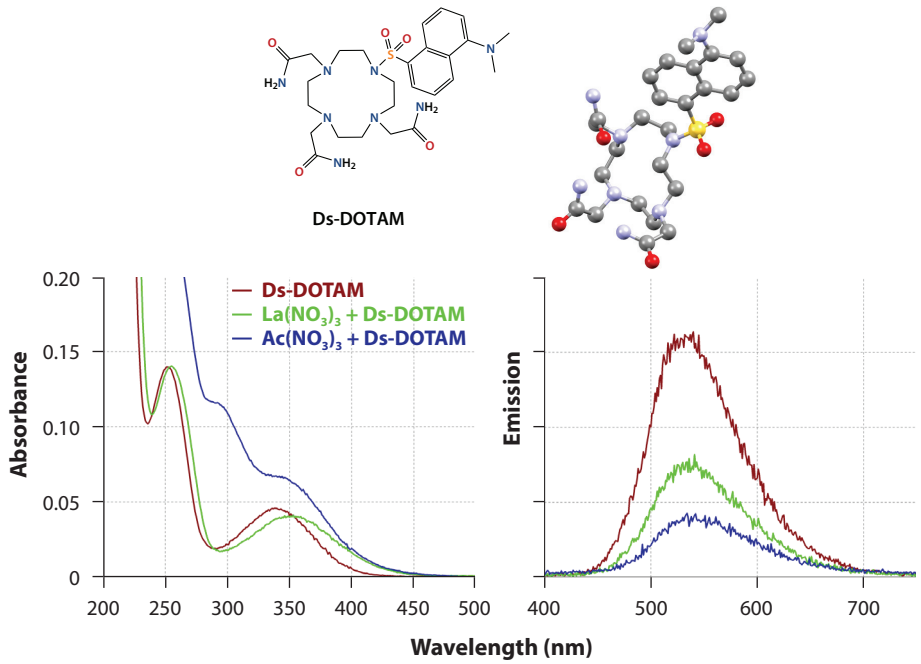

Figure 3. The new fluorescent ligand, Ds-DOTAM, shown with a solid-state structure determined by single-crystal X-ray diffraction studies (*top*). The UV-vis. absorbance (*bottom left*) and emission (*bottom right*) spectra of Ds-DOTAM upon the addition of excess $La(NO_3)_3$ and $Ac(NO_3)_3$ (La^{3+} is the $4f^0$ analog of the $5f^0$ species Ac^{3+}). The spectrum of the Ac^{3+} sample is partially obscured by the presence of excess nitrate ions, which gives rise to the absorbance feature at 290 nm. The emission spectra show similar quenching efficiencies of La^{3+} and Ac^{3+}, indicating that they both interact with Ds-DOTAM.

be different for the two ions, which possess substantially different ionic radii. To ascertain structural aspects of Ac chemistry, we directed efforts toward X-ray absorption spectroscopy (i.e., X-ray absorption near edge structure, XANES, and extended X-ray absorption fine structure, EXAFS), using high intensity synchrotron sources coupled with fluorescence detection methods.

Analyzing a small quantity of ^{227}Ac with these methods gave a significant edge-rise at 15.87 keV (Fig. 4). This energy corresponds to the L_{III} edge of Ac, and is therefore diagnostic of this element. Although the XANES region is not expected to yield a large amount of information about the non-redox-active Ac^{3+} ion, the EXAFS region can inform us about Ac-ligand interatomic distances. For this particular sample, Ac^{3+} was dissolved in 0.1 M ammonium acetate pH 5 buffer. These conditions mimic those used to create therapeutically relevant ^{225}Ac-labeled antibodies, and can therefore shed light on the speciation and nature of Ac^{3+} prior to conjugation.

In conjunction with DFT and molecular dynamics calculations, EXAFS data analysis is underway. These data represent the first X-ray absorption spectra of Ac, and will enable the determination of Ac-ligand interatomic distances and coordination numbers in the solution phase for the first time (see article by Stein & Kerlin).

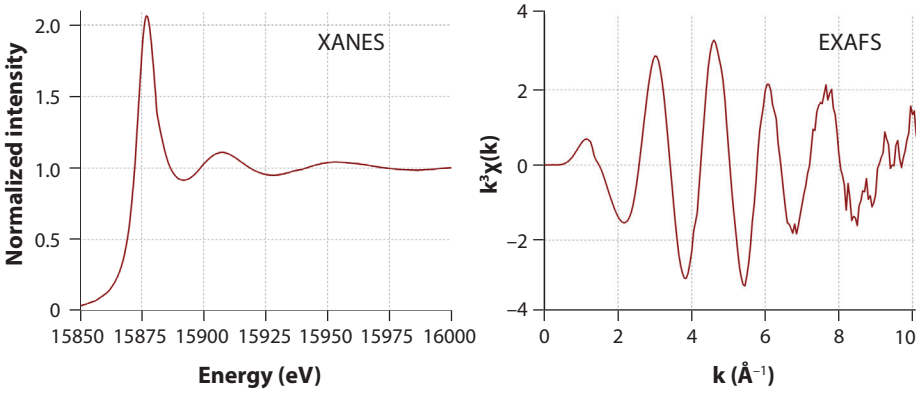

Figure 4. XANES (*left*) and EXAFS (*right*) L_{III} edge spectra of $^{227}Ac^{3+}$ (2 mCi in 0.45 mL, 270 µM) in 0.1 M ammonium acetate pH 5 buffer. These data show good intensity, indicating that EXAFS provides a viable path for characterizing structural aspects of Ac^{3+} coordination complexes.

Summary

For the first time in over 50 years, the chemistry of actinium is under active exploration by researchers at Los Alamos National Laboratory (LANL). This effort is motivated by the great therapeutic potential of ^{225}Ac, the clinical development of which is currently limited by a lack of knowledge of the fundamental coordination chemistry of this element. Our research has thus far demonstrated that Ac^{3+} is generally averse to interacting with nitrogen donor ligands. We have also shown that fluorescence spectroscopy can be used to interrogate Ac-ligand binding, and that 2 mCi quantities of ^{227}Ac provide sufficient signal to obtain EXAFS spectra from which interatomic distances and coordination numbers can be obtained. These results provide a strong foundation for the continued exploration of Ac chemistry. The data obtained from these efforts will have direct application in the design of better ligands for Ac^{3+}, leading to safer, more effective ^{225}Ac-based radiopharmaceutical agents.

Further reading:

1. *S. Fried, F. Hagemann, and W. H. Zachariasen, "The preparation and identification of some pure actinium compounds", J. Am. Chem. Soc. 1950, 72, 771-75.*
2. *J. G. Stites, M. L. Salutsky, and B. D. Stone, "Preparation of actinium metal", J. Am. Chem. Soc. 1955, 77, 237-40.*
3. *J. D. Farr, A. L. Giorgi, M. G. Bowman, and R. K. Money, "The crystal structure of actinium metal and actinium hydride", J. Inorg. Nucl. Chem. 1961, 18, 42-47.*
4. *F. Weigel, and H. Hauske, "The lattice constants of actinium(III) oxalate deca-hydrate", J. Less-Common Met. 1977, 55, 243-47.*
5. *K. A. Deal, I. A. Davis, S. Mirzadeh, S. J. Kennel, and M. W. Brechbiel, "Improved in vivo stability of actinium-225 macrocyclic complexes", J. Med. Chem. 1999, 42, 2988-92.*
6. *M. R. McDevitt, D. Ma, L. T. Lai, J. Simon, P. Borchardt, R. K. Frank, K. Wu, V. Pelligrini, M. J. Curcio, M. Miederer, N. H. Bander, and D. A. Scheinberg, "Tumor therapy with targeted atomic nanogenerators", Science 2001, 294, 1537-40.*
7. *M. R. McDevitt, D. Ma, J. Simon, R. K. Frank, and D. A. Scheinberg, "Design and synthesis of ^{225}Ac radioimmunopharmaceuticals", Appl. Radiat. Isot. 2002, 57, 841-47.*
8. *H. Kirby, and L. Morss, "Actinium", in: L. Morss, N. Edelstein, J. Fuger (Eds.) The Chemistry of the Actinide and Transactinide Elements, Springer Netherlands, 2006, pp. 18-51.*
9. *M. Miederer, D. A. Scheinberg, and M. R. McDevitt, "Realizing the potential of the Actinium-225 radionuclide generator in targeted alpha particle therapy applications", Adv. Drug Delivery Rev. 2008, 60, 1371-82.*
10. *D. A. Scheinberg, and M. R. McDevitt, "Actinium-225 in targeted alpha-particle therapeutic applications", Curr. Radiopharm. 2011, 4, 306-20.*
11. *J. J. Wilson, E. R. Birnbaum, E. R. Batista, R. L. Martin, and K. D. John, "Synthesis and characterization of nitrogen-rich macrocyclic ligands and an investigation of their coordination chemistry with lanthanum(III)", Inorg. Chem. 2015, 54, 97-109.*
12. *J. J. Wilson, M. Ferrier, V. Radchenko, J. R. Maassen, J. W. Engle, E. R. Batista, R. L. Martin, F. M. Nortier, M. E. Fassbender, K. D. John, and E. R. Birnbaum, "Evaluation of nitrogen-rich macrocyclic ligands for the chelation of therapeutic bismuth radioisotopes", Nucl. Med. Biol. 2015, 42, 428-38.*
13. *G. Thiabaud, V. Radchenko, J. J. Wilson, K. D. John, E. R. Birnbaum, and J. L. Sessler, "Rapid insertion of bismuth radioactive isotopes into texaphyrin in aqueous media", J. Porphyr. Phthalocyanines 2017, 21, 12, 882-886.*
14. *N. A. Thiele, V. Brown, J. M. Kelly, A. Amor-Coarasa, U. Jermilova, S. N. MacMillan, A. Nikolopoulou, S. Ponnala, C. F. Ramogida, A. K. H. Robertson, C. Rodríguez-Rodríguez, P. Schaffer, C. Williams Jr., J. W. Babich, V. Radchenko, and J. J. Wilson, "An Eighteen-Membered Macrocyclic Ligand for Actinium-225 Targeted Alpha Therapy", Angew. Chem. Int. Ed. 2017, 56, 14712–14717.*
15. *N. A. Thiele, and J. J. Wilson, "Actinium-225 for Targeted α Therapy: Coordination Chemistry and Current Chelation Approaches", Cancer Biother. Radiopharm. 2018, 33, 336-48.*

Acknowledgments

This work is a collaborative effort with several others researchers: Beau J. Barker, Enrique R. Batista, John M. Berg, Eva R. Birnbaum, Jonathan W. Engle, Michael E. Fassbender, Maryline G. Kerlin, Kevin D. John, Stosh A. Kozimor, Joel R. Maassen, Richard L. Martin, F. Meiring Nortier, Valery Radchenko, and Marianne P. Wilkerson all contributed and played vital roles in initiating and contributing to this ongoing project. Financial support was provided by the U.S. Department of Energy through the LANL/LDRD program and the Seaborg Institute for the postdoctoral fellowship to Dr. Wilson.

Spectroscopic Studies of Highly Radioactive Elements Relevant to Targeted Alpha Therapy

Understanding the chemistry of trivalent (3+ charge) actinides represents a longstanding challenge in f-element chemistry. This area of research is important for solving numerous technical problems that can influence our quality of life. Consider the role actinide(III) cations play in terms of targeted alpha therapy, nuclear waste storage and treatment, maintaining energy security, and improving global security. However, with the exception of U^{3+}, the early-to-mid-actinides in the +3 oxidation state (An = Ac^{3+}, Np^{3+}, Pu^{3+}, Am^{3+}, Cm^{3+}, Bk^{3+}, and Cf^{3+}) are virtually unexplored. This is largely due to barriers that are faced studying these elements, such as safely handling highly radioactive samples, limited access to materials of interest, and redox instability of some An^{3+} ions (e.g., Np and Pu).

Actinium-225 as an anti-cancer agent

This clear need to advance our understanding of actinides has inspired many researchers to advance the chemistry and physics of actinide(III) cations. One area of research where Los Alamos National Laboratory (LANL) provides leadership and innovation is associated with using ^{225}Ac in targeted alpha therapeutic treatment of disease. The ^{225}Ac isotope is attractive because its alpha decay deposits large amounts of energy (>5 MeV; Fig. 1) over a short range in biological tissue. Hence, targeted delivery of ^{225}Ac to a diseased cell offers an opportunity to selectively kill the unhealthy cell and leave surrounding healthy tissue unharmed (see Fig. 1 in article by Wilson on p2). The major chemical challenge associated with this technology is related to targeting of Ac^{3+}. A proper Ac^{3+} chelate—an organic molecule capable of holding onto ^{225}Ac while it is delivered through the body—is required. Unfortunately, there is insufficient fundamental chemistry known for Ac^{3+} to rationally design an appropriate chelating agent. Note that there are only a handful of coordination chemistry studies on actinium (Ac), most of which were carried out during the Manhattan project or the years shortly after.

Armed with a unique national resource—160 micrograms of the longest-lived isotope of actinium, ^{227}Ac ($t_{½}$ = 21.77 y)—we embarked on a quest to carry out vital fundamental studies that advance Ac^{3+} coordination chemistry in support of chelate design. This effort has been supported by the Department of Energy (DOE) Heavy Element Chemistry program, DOE Nuclear Physics, LANL Laboratory Directed Research and Development (LDRD) Exploratory Research (ER) and Directed Research (DR) programs, the Seaborg Institute, the Office of Science Graduate Student Research fellowships, and the Stanford Synchrotron Radiation Lightsource (SSRL) and Advanced Light Source (ALS) DOE-supported synchrotron facilities. In a relatively short time (~three years) we have made substantial progress toward this goal. Members of our team successfully developed the capability to safely and reliably synthesize Ac^{3+} coordination compounds, characterize the Ac^{3+} reaction products using a wide range of spectroscopic techniques, and model the physical and chemical properties of Ac^{3+} compounds using advanced state-of-the-art computational methodologies.

Benjamin Stein

Benjamin Stein was a Seaborg Institute Postdoctoral Research Fellow from July 2015 to April 2018 working under the mentorship of Stosh Kozimor. He is currently a technical staff member in the Physical Chemistry and Applied Spectroscopy group (C-PCS). His research interests lie in the development of spectroscopic methods for the characterization of actinide systems.

Maryline Kerlin

Maryline Kerlin (née Ferrier) was a Glenn T. Seaborg Institute Postdoctoral Research Fellow from February 2015 to September 2017 under the mentorship of Stosh Kozimor. She is currently at the University of Washington Seattle as a senior postdoctoral fellow in the School of Medicine. Her research interests reside in radiochemistry and basic fundamental chemistry of actinides.

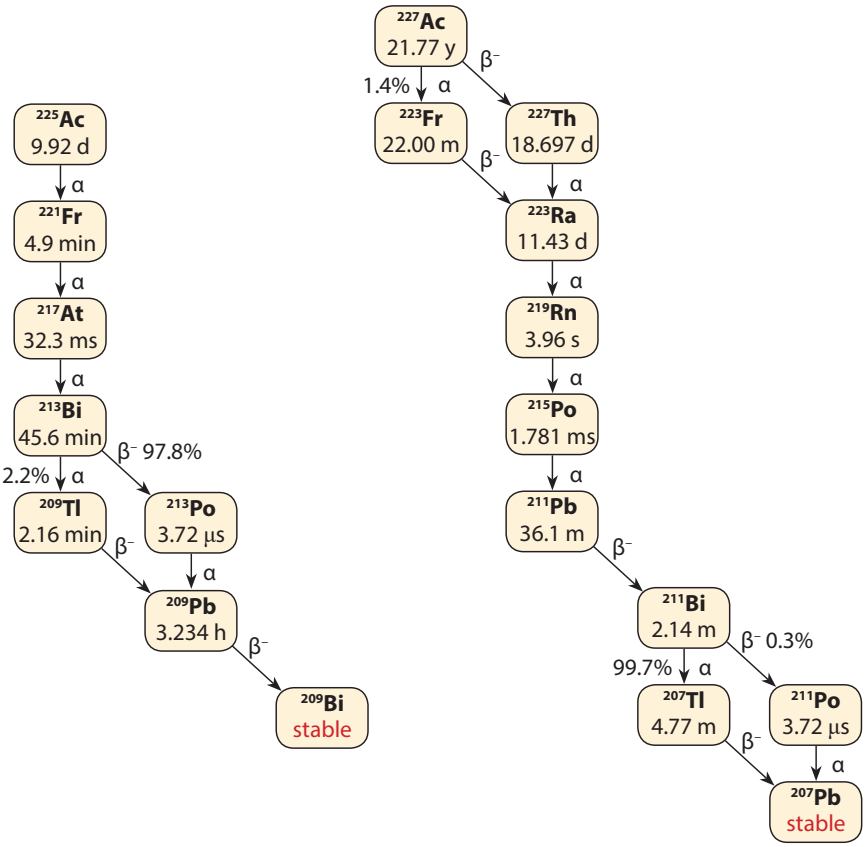

Figure 1. Radioactive decay chains of ^{225}Ac (*left*) and ^{227}Ac (*right*). Note the four alpha particles emitted during the decay of the short-lived ^{225}Ac, which are responsible for the high effectiveness of this isotope in clinical use.

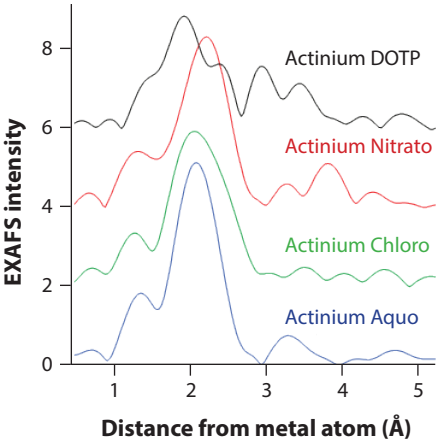

Figure 2. Extended X-ray absorption fine structure (EXAFS) spectra of Ac coordination complexes. The position on the x-axis is related to the distance of the ligand from the metal atom, while the intensity is related to the number and atomic number, *Z*, of the scattering atom(s). These data can give information on the bonding environment in the metal complexes. In particular, the number of water molecules bound in $Ac(H_2O)_x^{3+}$ can be estimated, an important parameter for predicting the behavior of Ac^{3+} in aqueous solution.

Spectroscopic characterization

Success with our initial "proof-of-concept" experiments (see article by Wilson in this issue, p2) demonstrated that extended X-ray absorption fine structure (EXAFS) measurements were feasible. Encouraged by these results, which have required use of a synchrotron facility, our first measurements focused on characterizing a series of basic Ac^{3+} complexes that contained inorganic ligands. In addition to being able to synthesize, characterize, and computationally model the molecular dynamics of the desired Ac^{3+} complexes, we developed methods to recover the precious ^{227}Ac isotope from the used samples for future studies. This work has provided the first ever X-ray absorption measurements on Ac and has enabled Ac–ligand bond distances to be measured for the first time. Moreover, these results established confidence and credibility for characterization of more complicated Ac–ligand interactions, like those associated with medically relevant chelators.

Ac-aquo complexes

Our initial efforts focused on characterizing the simple Ac-aquo complex, i.e., Ac^{3+} complexed by only water molecules. The Ac-aquo ion was selected for study because metal-aquo ions occupy central roles in all equilibria that define metal complexation in natural environments. These complexes are typically used to establish thermodynamic metrics (such as stability constants) for predicting metal-ligand binding and equilibria. They are essential for defining critical parameters associated with aqueous speciation, metal chelation, in vivo transport, and so on. These constants were acquired for most metals by the mid-twentieth century—it is a testament to the actinide knowledge gap that we still do not possess this data. As such, establishing the fundamental chemistry of the Ac-aquo ion, $Ac(H_2O)_x^{3+}$, is critical for current efforts to develop ^{225}Ac as a targeted anticancer therapeutic agent.

The Ac L_3-edge EXAFS studies (Fig. 2) revealed 10.9(5) water molecules directly coordinated to the Ac^{3+} cation with an Ac–O_{H_2O} distance of 2.63(1) Å (where the number in parentheses denotes the uncertainty in the last digit). This experimentally-determined distance was broadly consistent with molecular dynamics-density functional theory calculations that showed Ac^{3+} coordinated by an average of nine water molecules with Ac–O_{H_2O} distances ranging from 2.61 to 2.76 Å. Note that this discrepancy may arise from several sources, including difficulties in computationally modeling the complex aqueous environment. However, experimental data on challenging systems such as these are crucial for improving the predictive capability of quantum chemical methods. Moreover, these data paved the way for subsequent efforts to characterize substitution reactions on the metal using various ligands in aqueous media. Knowledge of this fundamental speciation behavior has subsequently allowed us to understand the fundamental inorganic chemistry of chloro and nitrato Ac complexes, for instance, and has provided us with the spectroscopic toolbox necessary to study more complicated metal-chelate systems. These include chelators relevant to the application of alpha-emitting radioisotopes in medicine.

Coordination chemistry of Ac^{3+} with macrocyclic ligands

Emboldened by these successes, we subsequently shifted focus to characterizing Ac^{3+} interactions with complex chelates relevant to medical applications. We began with the DOTA chelate (Fig. 3), one of the most common ligands used for the chelation of radiometals (including some clinical work with Ac^{3+}). Our results were consistent with numerous clinical and pre-clinical studies that showed DOTA labeling efficiency is low and that the binding kinetics for forming an Ac-DOTA complex are slow. In addition, our nuclear magnetic resonance (NMR) and EXAFS studies suggested that the DOTA binding pocket is too small for the large Ac^{3+} cation. To achieve high labeling efficiencies and faster binding kinetics we began studies of the DOTP chelate. This ligand differs from DOTA in that the acetates have been replaced by phosphonates (Fig. 3). This small change imparts numerous attractive attributes over DOTA—for example, phosphonates are known to bind f-elements quite well, and there are several phosphonates used as extractants in actinide and

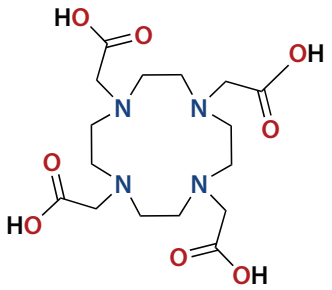

DOTA

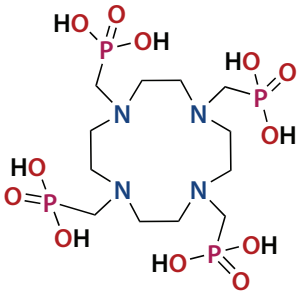

DOTP

Figure 3. DOTA (*top*), DOTP (*bottom*), the two metal chelators (ligands) discussed in this article. The work by Wilson described in the previous article concluded that oxygen atom donors are preferable to nitrogen.

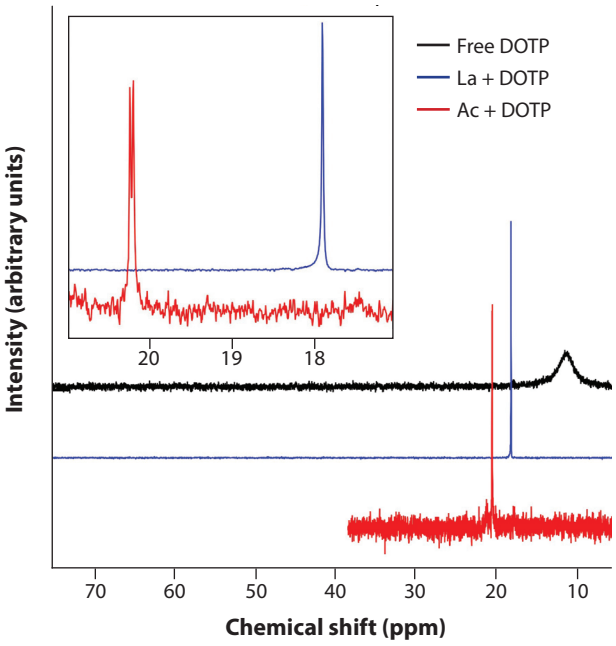

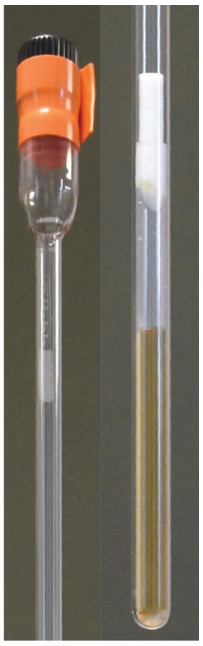

Figure 4. *Left*: Phosphorus-31 NMR spectra of free (unbound) DOTP ligand (black), lanthanum DOTP complex (blue), and Ac-DOTP complex (red). *Right*: Sample containment for radioactive samples. To safely contain the sample, a nested arrangement of Teflon and Pyrex tubes are used. This is the first recorded NMR spectrum for an Ac complex, and shows characteristic signals that can be used to identify the different species in solution.

Acknowledgments

BWS would like to thank Stosh Kozimor (C-IIAC), Eva Birnbaum (SPO-SC), John Berg (AMPP-4) for their excellent support and guidance throughout their postdoctoral tenure. Additionally, large portions of this work would not have been possible without the expertise of our collaborators in T-division, including Ping Yang (T-1) and Enrique Batista (T-CNLS). Other collaborators for this work include Samantha Cary, Sharon Bone (SSRL), and Juan Lezama Pacheco (SSRL). BWS gratefully acknowledges the Los Alamos Glenn T. Seaborg Institute for postdoctoral fellowship funding. Research presented in this article was supported by the LDRD program of LANL under project numbers 20150575ER, 20180005DR, and 20150646DR. The author also thanks the Hoffman Distinguished Postdoctoral Fellowship (Cary) and the Agnew National Security Fellowship (Bone). We recognize additional support from the Heavy Element Chemistry Program at LANL by the U.S. Department of Energy Office of Science Basic Energy Sciences Program. We acknowledge the United States Department of Energy, Office of Science, Isotope Development and Production for Research and Application subprogram within Office of Nuclear Physics for their support in supplying the ^{227}Ac and ^{243}Am isotopes. Use of the Stanford Synchrotron Radiation Lightsource, SLAC National Accelerator Laboratory, was supported by the U.S. Department of Energy, Office of Science, Office of Basic Energy Sciences under Contract No. DE-AC02-76SF00515. The SSRL Structural Molecular Biology Program is supported by the DOE Office of Biological and Environmental Research, and by the National Institutes of Health, National Institute of General Medical Sciences (including P41GM103393).

lanthanide purifications. In addition, the C–phosphonate bond (in DOTP) is longer than the C–acetate bond (in DOTA). This characteristic gives DOTP a slightly larger "pocket" for binding Ac^{3+}. From a spectroscopic point of view, the phosphorus atoms are also attractive—they provide an excellent spectroscopic handle for both NMR spectroscopy (Fig. 4) and EXAFS. The ^{31}P nucleus is directly detectable by NMR, which consequently enabled us to collect the first NMR spectra for an Ac compound. The heavy phosphorus atoms also provide good scattering signals in EXAFS measurements, which facilitates spectral interpretations.

Our recent investigation using Ac^{3+} and DOTP suggested that the DOTP ligand may be superior to DOTA on numerous fronts. The NMR data indicated that DOTP binds Ac^{3+} quantitatively to form a single species, a result confirmed by EXAFS. Moreover, Ac–binding appears to be quite rapid (minutes) at room temperature and under mild chemical conditions. This is important, as biological targeting vectors such as antibodies are unable to resist high temperature without compromising their targeting efficacy. Encouraged by these results, current efforts are focused on quantitatively characterizing the labeling efficiencies and binding kinetics. We have embarked on a campaign to characterize the use of DOTP for in vitro and in vivo applications.

Outlook and future studies

These studies show the first examples of EXAFS and NMR characterization of Ac^{3+} coordination chemistry. Furthermore, we have demonstrated the potential utility of the phosphonate class of chelators for Ac^{3+} coordination. Several studies are ongoing at LANL to further explore this potential, spanning Biology (B), Chemistry (C), and Theory (T) divisions. With this powerful spectroscopic capability in hand we are now planning future studies of both the complexation by simple biologically-relevant anions, such as phosphate and carbonate, in addition to other chelators. Of particular interest are chelators that show potential to "hold-onto" Ac^{3+} once bound to biological targeting vectors for subsequent in-vitro and in-vivo experimentation.

Further reading:

1. *Y.-S. Kim, and M. W. Brechbiel, "An Overview of Targeted Alpha Therapy", Tumor Biol., 2012, 33 (3), 573.*
2. *J. N. Mathur, M. S. Murali, and K. L. Nash, "Actinide Partitioning—a Review", Solvent Extr. Ion Exch., 2001, 19 (3), 357.*
3. *P. Paviet-Hartmann, G. Cerefice, M. Stacey, and S. Bakhtiar, "Analysis of Nuclear Proliferation Resistance Reprocessing and Recycling Technologies", United States, 2011*
4. *H. W. Kirby, and L. R. Morss, "Actinium", The chemistry of the actinide and transactinide elements, Springer, 2006, 18-51.*
5. *M. G. Ferrier, E. R. Batista, J. M. Berg, E. R. Birnbaum, J. N. Cross, J. W. Engle, H. S. La Pierre, S. A. Kozimor, J. S. Lezama Pacheco, B. W. Stein et al., "Spectroscopic and Computational Investigation of Actinium Coordination Chemistry", Nat. Commun., 2016, 7, 12312.*
6. *M. G. Ferrier, B. W. Stein, E. R. Batista, J. M. Berg, E. R. Birnbaum, J. W. Engle, K. D. John, S. A. Kozimor, J. S. Lezama Pacheco and L. N. Redman, "Synthesis and Characterization of the Actinium Aquo Ion", ACS Cent. Sci., 2017, 3 (3), 176.*
7. *M. G. Ferrier, B. W. Stein, S. E. Bone, S. K. Cary, A. S. Ditter, S. A. Kozimor, J. S. L. Pacheco, V. Mocko, G. T. Seidler, "The Coordination Chemistry of CmIII , AmIII , and AcIII in Nitrate Solutions: an Actinide L_3 -Edge EXAFS Study", Chem. Sci., 2018, 9 (35), 7078.*
8. *A. L. Morgenstern, B. W. Stein, M. G. Ferrier, E. R. Batista, S. E. Bone, S. K. Cary, K. D. John, B. L. Scott, J. S. L. Pacheco, E. R. Birnbaum, S. A. Kozimor, V. Mocko and P. Yang, "Chelating +3 Metals (La, Ac, Am, Cm) with H_8DOTP; 1,4,7,10-Tetraazacyclododecane-1,4,7,10-Tetra(methylene) Phosphonic Acid", manuscript in preparation.*

Probing Covalency in f-Element Compounds: A Theoretical Study of X-Ray Absorption Spectra of Americium and Europium Chlorides

A detailed understanding of chemical bonding in f-element compounds should allow us to develop effective extractants for the separation of minor actinides (e.g., Am, Cm) from lanthanides in advanced fuel cycles. This objective remains challenging due to their similar ionic radii and chemical behavior. One fundamental difference between these elements is that lanthanide (Ln) 4f orbitals are core-like and strongly localized, whereas actinide (An) 5f orbitals have a larger radial extension. These differences lead to a difference in metal-ligand bonding covalency, which in principle can lead to differences in separation efficiency. Quantifying these differences in covalency, however, is still a problematic issue that stimulates much debate.

X-ray absorption spectroscopy (XAS) coupled with first-principle modeling has emerged as a powerful combination of techniques for characterizing electronic structure and covalent bonding. However, the theoretical prediction of these compounds' spectra with multiple unpaired f-electrons is complicated due to complex effects such as the large number of excited states involved, spin-orbit (SO) coupling, and appreciable multiplet effects. Density functional theory (DFT), with its balance between accuracy and computational cost, has become a popular approach for calculating molecular electronic structures and spectra. In this article, we report our DFT studies on the electronic structure and simulation of XAS spectra of Am(III) and Eu(III) compounds with $5f^6$ and $4f^6$ states, respectively. These particular elements were chosen to study because they are valence isoelectronic (i.e., they possess the same number electrons in their outer "valence" shell), they are both involved in the actinide separation, and they were featured in a famous ion-exchange study by Seaborg and coworkers in the 1950s. The covalency of the isoelectronic Am/Eu–Cl bond has been compared and discussed.

Seaborg ion-exchange study

Differences in the chemical behavior between actinide and lanthanide elements were first observed by Glenn Seaborg and coworkers in the 1950s. Performing a cation-exchange resin elution with trivalent actinide (Ac, Pu, Am, Cm) and lanthanide (La, Ce, Pm, Eu, Yb) elements using hydrochloric (HCl) acid solution, they demonstrated that the actinides had faster elution rates than the lanthanides at higher HCl concentrations. A suggested explanation of the transuranium ions' unique behavior was that in high concentrations of acid, the actinides form complex ions with chloride ions to a greater extent than the lanthanides due to partial covalent bonding using 5f orbitals. Since this discovery, 5f versus 4f covalency has been a fundamental concern, and is still hotly debated. The motivation of this research was

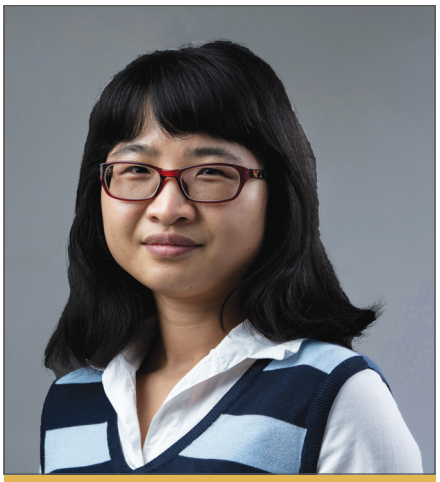

Jing Su

Jing Su was a Seaborg Institute Postdoctoral Research Fellow from October 2015 to September 2017, working under the mentorship of Ping Yang and Enrique Batista. The subject of her work was high-level theoretical studies of actinide-ligand bonding interactions. She is currently a postdoctoral fellow in the T-1 group at LANL.

*«« **Covalency** is a component of a chemical bond in which electrons are shared between atoms in molecular orbitals. These orbitals are formed from mixing atomic orbitals of the appropriate symmetry. It constitutes a minor part of f-orbital bond mixing in comparison to the ionic (Coulombic) forces.*

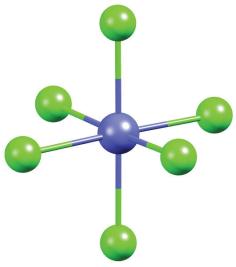

Figure 1. Representation of $(PPh_4)_3AmCl_6$ crystal structure; PPh_4^+ cations (omitted) do not coordinate to the actinide, their role is to balance the charge with the $AmCl_6^{3-}$ trianion.

Atomic Model 101

The structure of an atom consists of negatively charged electrons in a field around a positively charged nucleus. Electrons are quantum particles and do not move around objects in the way, for instance, planets rotate around the Sun. Instead, they are found in probabilistic orbitals, occupied by a limited number of electrons and labeled from simplest to most complex by their symmetry as s, p, d, and f (short for "sharp", "principal", "diffuse", and "fundamental", respectively, originating from the appearance of corresponding lines in atomic spectroscopy; *see illustration below*).

As the electrons pair up in these orbitals, they fill successive shells as the periodic table is traversed, indicated by a label known as the principal quantum number (e.g., "3p" refers to the p orbital in the third shell). A filled shell is generally inert—chemists are most interested in the outer, unfilled shell, which is known as the "valence" shell.

The f orbitals are only accessed by heavier elements such as the lanthanides and actinides (4f and 5f, respectively—the first f orbital has a principal quantum number of 4 as it is fourth in the s, p, d, f series). They remain poorly understood due to their complexity and contracted nature, which limits measurable bonding interactions between adjacent atoms.

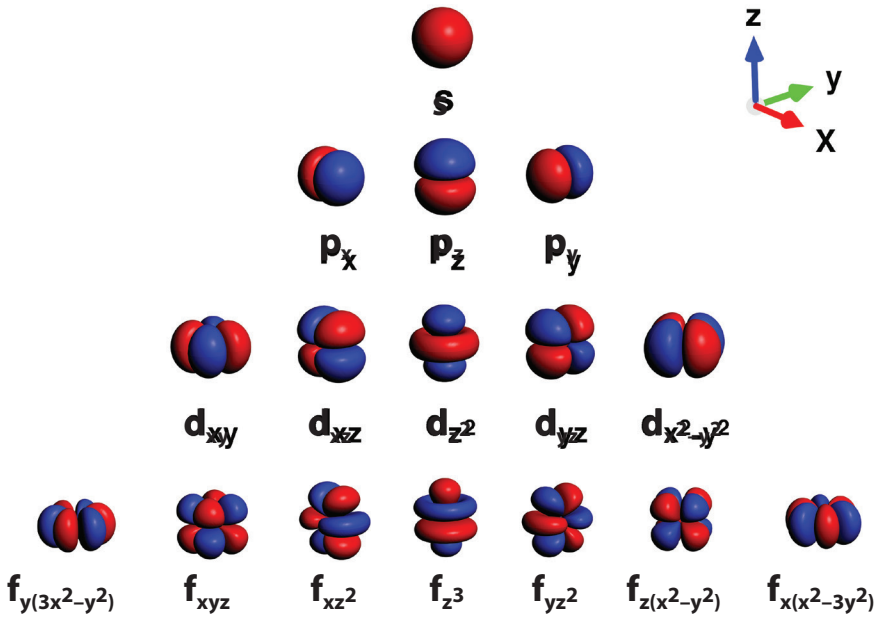

Figure 2. The spatial extent of the 1s, 2p, 3d and 4f orbitals, showing increasing complexity and planes of symmetry through the series. The f electrons are only accessed by heavier elements such as the lanthanides and actinides. Each of these orbitals can accommodate two electrons, each with diametrically opposed spins.

therefore to resolve this important issue by examining some of the proposed species invoked in Seaborg's original work.

Approach

The relative participation of 6d vs. 5d and that of 5f vs. 4f in the M–Cl bond was assessed. We did this by determing the amount of mixing between both the metal 5f and 6d orbitals and the Cl 3p orbital in $AmCl_6^{3-}$, and in a similar manner comparing the corresponding 4f and 5d mixing with Cl 3p in $EuCl_6^{3-}$.

Generally, the d orbitals, which have greater extension than their f orbital congeners, are the basis of much of the covalent bonding in metals. However, we expect that measuring the differences between 5f and 4f mixing with Cl 3p is key to understanding the differences between Am-Cl and Eu-Cl bond covalency. In this joint effort between theoretical and experimental approaches, the synthesis, characterization, and Cl K-edge XAS measurements (see Fig. 3 for their principle) were carried out by our collaborators at Los Alamos National Laboratory (LANL) and University of California, Irvine. Concurrently, we performed a series of DFT calculations to simulate the experimental spectra, providing essential insights into the nature of the Am/Eu–Cl bonds.

Molecular orbital (MO) scheme

The crystal structure of $(PPh_4)_3AmCl_6$ shows that $AmCl_6^{3-}$ forms a slightly distorted octahedron (Fig. 1, previous spread). Two geometries of $AmCl_6^{3-}$ were used in the calculations to interpret the XAS spectra: perfect octahedral (O_h) symmetry and the experimental crystal structure coordinates. As both calculations gave similar results in many cases, for clarity we exploited the simplicity of the high-symmetry O_h calculation when describing the nature of the orbitals. The valence molecular orbital (MO) scheme and contour diagram calculated using scalar-relativistic (SR) DFT are shown in Fig. 4, along with details of the interactions.

Spin-orbit (SO) coupling complicates MO picture

Making spin-orbit corrections in these calculations is important, despite the fact that they are small in energetic terms for the f shell, because the level splitting it induces can significantly affect the prediction of spectroscopic signatures. Relativistic effects, which include both scalar relativistic (SR) effects (due to mass-velocity and Darwin terms) and SO coupling effects, are appreciable in particular for Am, as it is a heavy element with an unfilled 5f shell. Therefore, SO effects were included as a correction to the SR results.

As depicted in Fig. 5, SO coupling changes the MO picture in two notable ways. First, the orbital energy degeneracy was substantially decreased (degeneracy refers to the number of orbitals of identical energy). Second, SO coupling causes appreciable mixing of SR molecular orbitals. Overall, these results exemplify how SO coupling, while improving the accuracy of the predictions, complicates the identification of M–Cl σ- from π-interactions in transitions measured by Cl K-edge XAS.

Comparison of simulated spectra using SR and SO methods

A direct comparison of simulated X-ray absorption spectra of $AmCl_6^{3-}$ at the SR and SO levels using experimental coordinates is shown in Fig. 6. The main differences in terms of both peak positions and intensities are found in the lower energy range of 2820–2824 eV, corresponding to electronic transitions to Am 5f orbitals. The lowest pre-edge feature from the SO-DFT simulation (2821.5 eV) is closer to the experimental result (2823.0 eV) compared with the SR-DFT simulation (2821.0 eV). The

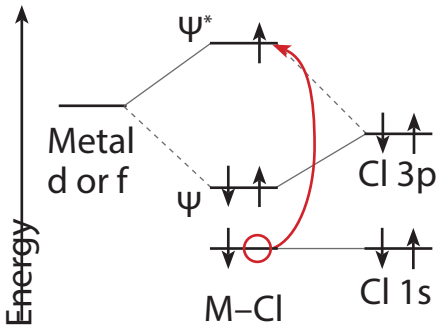

Figure 3. Illustration showing electronic excitations in a ligand K-edge X-ray absorption spectroscopy (XAS) experiment. The black arrows represent electrons, the horizontal lines show discrete energy levels, representing various molecular and atomic orbitals. The red arrow shows the excitation of a core Cl 1s electron into an unfilled molecular orbital resulting from the mixing of Cl 3p and metal valence d or f orbitals. This transition creates a characteristic absorption feature called the K-edge, which can be used to characterize metal-ligand orbital mixing coefficients using orbital descriptions. Because the core "hole" is localized on the absorbing Cl^- ligand, the dominant contribution to the transition dipole moment governing the intensity of these electronic transitions is directly related to the amount of Cl 3p character in the final state. Therefore, the Cl K-edge XAS experiment provides a direct gauge of covalency in M–Cl bonding (as defined by Heitler and London).

«« **Spin-orbit coupling** *is a phenomenon in which an unpaired electron's spin interacts with its own angular momentum. The origin of this effect is due to the electromagnetic interaction between the electron's magnetic dipole, its orbital motion, and the electrostatic field of the positively charged nucleus. It can shift the energy levels of orbitals within an atom or molecule.*

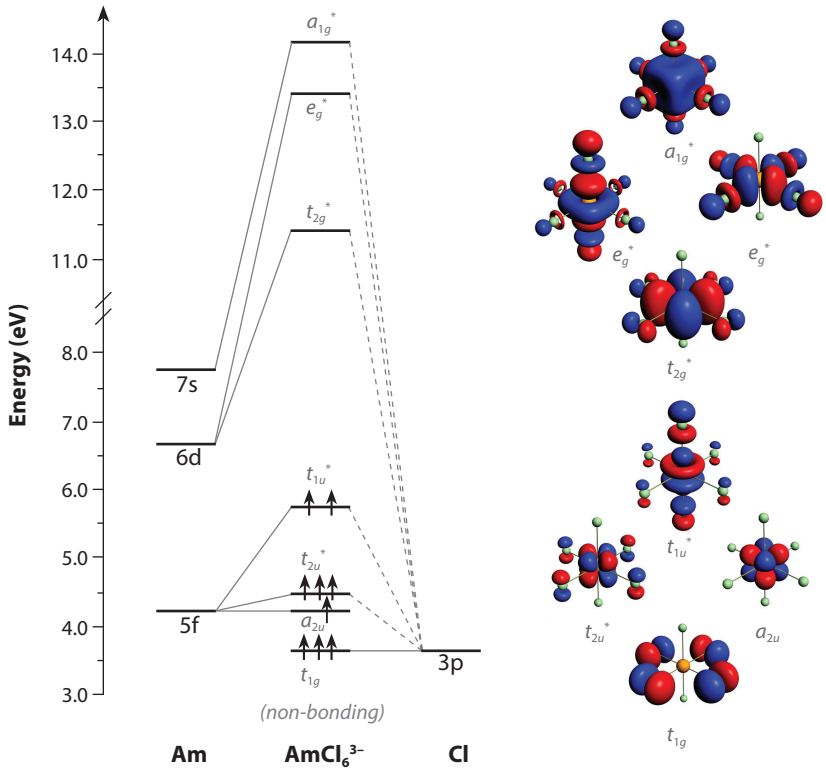

Figure 4. Molecular orbital energy levels (*left*) and contour diagrams of the O_h-$AmCl_6^{3-}$ ground state (*right*) calculated using scalar-relativistic DFT. This diagram shows the key orbitals involved in the Am–Cl bond. On the left of the energy level diagram are listed the atomic energy levels as solid horizontal lines of the 5f, 6d, and 7s orbitals in the isolated Am^{3+} ion; on the right is the 3p orbital of Cl^-. The energy levels in the center meanwhile represent the combined Am–Cl molecular orbitals in $AmCl_6^{3-}$ listed with their symmetry operators (asterisk denotes antibonding nature). The solid and dashed gray lines indicate the major and minor contributions from the atomic "parent" orbitals to the molecular orbitals, respectively.

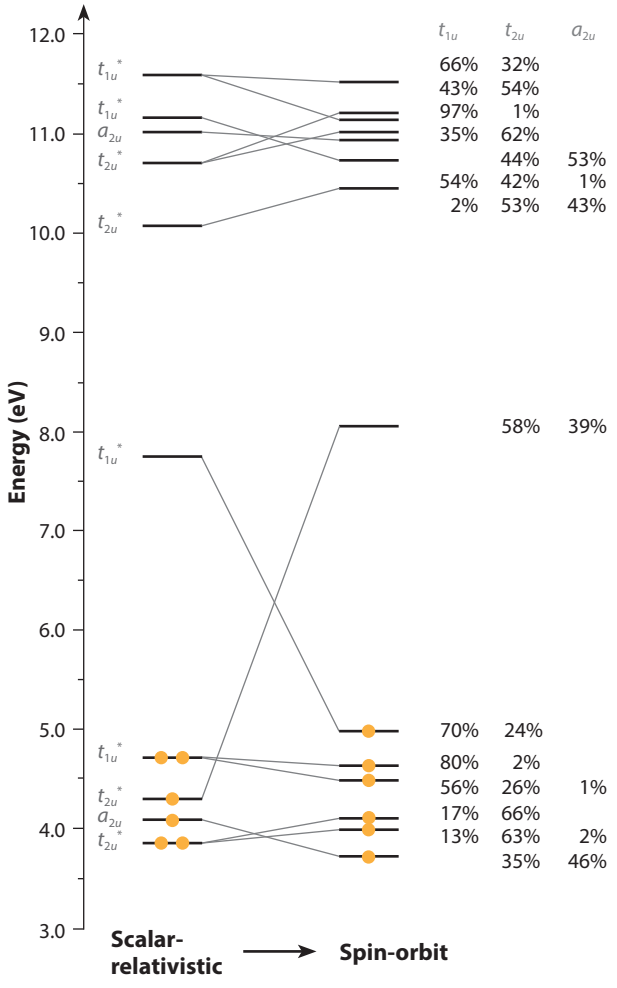

Figure 5. A diagram showing the energies for molecular orbitals from scalar-relativistic DFT calculations (*left*) versus those including spin-orbit coupling (*right*) for O_h-$AmCl_6^{3-}$. The orange dots represent unpaired electrons. This shows the significant effect of spin-orbit coupling for this actinide species, which changes some energy levels considerably after mixing with other orbitals (composition after mixing shown on right), including their relative order and removing degeneracies (i.e., splitting orbitals which previously shared identical energy levels).

high-lying orbitals (Am 6d, 7s and 7p) meanwhile are only marginally impacted by the inclusion of SO coupling because their angular momentum is smaller.

Similar results were observed for $EuCl_6^{3-}$. Hence, while the simple molecular orbital picture shown in Fig. 4 is valuable for a conceptual description of the $AmCl_6^{3-}$ orbital interactions and X-ray absorption spectra, its accuracy is limited for systems with multiple unpaired spins where SO effects are appreciable, even for the highly symmetric $AmCl_6^{3-}$ ($5f^6$) and $EuCl_6^{3-}$ ($4f^6$) octahedral anions.

Assessment of covalency

The simulated Cl K-edge X-ray absorption spectra for $AmCl_6^{3-}$ and $EuCl_6^{3-}$ at the SO-DFT level using experimental coordinates are presented in Fig. 7, in addition to experimental data. These results allow a direct evaluation of covalent M–Cl orbital mixing in $AmCl_6^{3-}$ and $EuCl_6^{3-}$, and reveal subtle differences in M–Cl covalent bonding.

Both theory and experiment indicate that d-contribution to bonding in both molecules is appreciable to a similar degree. The orbitals that result from metal d and chloride 3p orbital mixing contain 9–10% Cl 3p character. Both theoretical and experimental results agree that metal f orbital participation in covalent bonding is much smaller than for d orbitals. For $AmCl_6^{3-}$, mixing between Am 5f and Cl 3p orbitals is 0.54%. In contrast, for $EuCl_6^{3-}$, the amount of Cl 3p orbital mixing in the

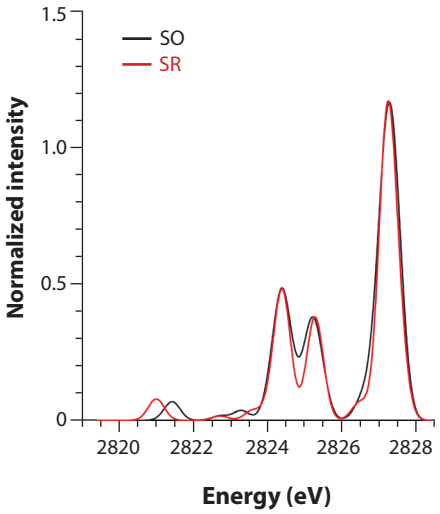

Figure 6. Transition dipole moment simulated Cl K-edge spectra of $AmCl_6^{3-}$ at the scalar-relativistic (SR) and spin-orbit (SO) levels.

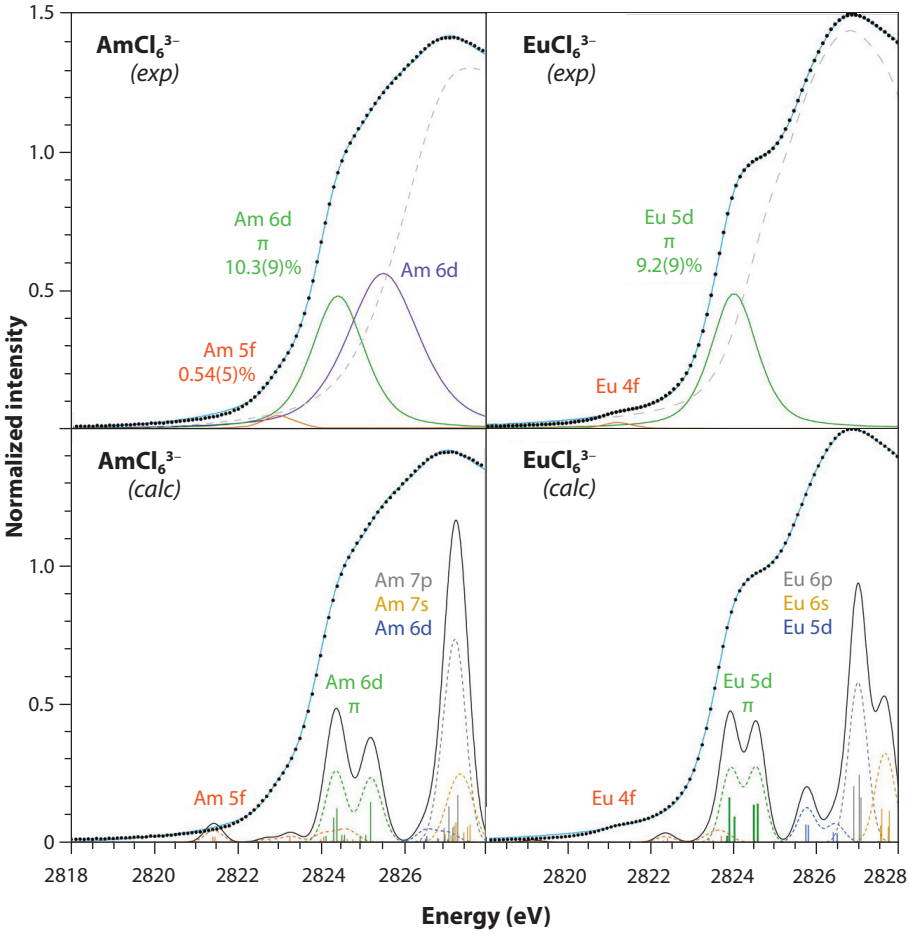

Figure 7. The experimental data (•) and the curve-fitted model (light blue trace) for the Cl K-edge XAS spectra from $(PPh_4)_3AmCl_6$ (in the two left-hand spectra) and $(PPh_4)_3EuCl_6$ (in the two right-hand spectra).

Top panels: The pre-edge pseudo-Voigt functions (orange, green, and purple traces) used to generate the curve-fitted model for the experimental data (•). Functions used to describe the edge region of the experimental Cl K-edge XAS spectrum have been summed and are represented as a dashed grey trace.

Bottom panels: Comparison between the experimental Cl K-edge XAS spectrum (•) and transition dipole DFT calculations (black trace). The orange, green, blue, yellow and grey bars and dashed traces represent the energy and oscillator strength for the DFT calculated transitions involving 5f, 6d, 7s and 7p final states, as shown. These dashed traces represent the individual contributions to the black trace.

Eu–Cl bond is too small to quantify and significantly less than that for $AmCl_6^{3-}$. The increase in Am–Cl orbital mixing likely results from the larger radial extension (0.5 Å) of the Am 5f orbitals with respect to Eu 4f orbitals.

While we recognize that the differences in M–Cl orbital mixing are subtle, we also acknowledge that small changes in covalency have the potential to appreciably influence chemical reactivity and physical properties. For example, an energy difference of only ~0.4 kcal/mol per bond is needed to achieve appreciable Am/Eu separations. While it is difficult to determine if the magnitude of this value is within the small orbital mixing differences we observed between $AmCl_6^{3-}$ and $EuCl_6^{3-}$, many claims have rationalized unusual actinide behavior by invoking 5f covalency in actinide-ligand bonding.

Most notably, our results confirm Seaborg's controversial 1954 hypothesis that Am^{3+} 5f orbital covalency is more substantial than for Eu^{3+} 4f in hexachloride salts.

Summary

We have directly evaluated the covalent M–Cl orbital mixing in $AmCl_6^{3-}$ and $EuCl_6^{3-}$ based on Cl K-edge XAS measurements and DFT calculations. Our results enhance the understanding of covalency differences between 5f and 4f orbitals (i.e., the difference between lanthanide and actinide-based outer shell f orbitals), which is relevant to the separation of actinides from lanthanides in nuclear fuel recycling. Furthermore, this work serves as a basis for efforts using other americium compounds to identify mechanisms to further enhance 5f- and 6d-contributions to covalent bonding.

Acknowledgments

Jing Su gratefully acknowledges a Glenn T. Seaborg Institute postdoctoral Fellowship and also thanks her mentors Ping Yang and Enrique R. Batista for their help with research, writing, and presentation skills. The research described here was carried out by a multidisciplinary team that spans LANL and UCI expertise in theory, radiochemistry, synthesis, and spectroscopy. Members of the LANL team include Justin N. Cross, Enrique R. Batista, Samantha K. Cary, Stosh A. Kozimor, Veronika Mocko, Brian L. Scott, Benjamin W. Stein and Ping Yang; the UCI team includes Cory J. Windorff and William J. Evans. This work was supported under the Heavy Element Chemistry Program at LANL by the Division of Chemical Sciences, Geosciences, and Biosciences, Office of Basic Energy Sciences, the U.S. Department of Energy. Portions of this work were supported by Glenn T. Seaborg Institute postdoctoral Fellowship (Stein, Su), the Director's Postdoctoral Fellowship (Cross), LANL Marie Curie Fellowship (Cary).

Further reading:

1. *E. I. Solomon, B. Hedman, K. O. Hodgson, A. Dey, R. K. Szilagyi, "Ligand K-edge X-ray absorption spectroscopy: covalency of ligand-metal bonds", Coord. Chem. Rev., 2005, 249, 97–129.*
2. *R. M. Diamond, K. Street Jr., G. T. Seaborg, "An Ion-exchange Study of Possible Hybridized 5f Bonding in the Actinides", J. Am. Chem. Soc., 1954, 76 (6), 1461–1469.*
3. *W. Heitler, F. London, "Wechselwirkung neutraler Atome und homöopolare Bindung nach der Quantenmechanik", Z. Eur. Phys. J. A 1927, 44, 455–472.*
4. *J. N. Cross, J. Su, E. R. Batista, S. K. Cary, W. J. Evans, S. A. Kozimor, V. Mocko, B. L. Scott, B. W. Stein, C. J. Windorff, P. Yang, "Covalency in Americium(III) Hexachloride", J. Am. Chem. Soc., 2017, 139(25), 8667–8677.*
5. *P. Ball, "Seaborg's americium dispute put to bed 60 years later", Chemistry World, www.chemistryworld.com/news/seaborgs-americium-dispute-put-to-bed-60-years-later/3007640.article*

Expanding the Frontiers of Non-Aqueous Transuranic Molecular Chemistry: Characterizing the First Np=N Multiple Bond

Jessie L. Brown

Jessie Brown was a Seaborg Institute Postdoctoral Research Fellow from April 2014 to July 2015 under the mentorship of Andrew Gaunt, studying multiple bonding in transuranic elements. She is now an Assistant Professor in chemistry at Transylvania University in Lexington, Kentucky.

Establishing a comprehensive understanding of actinide chemistry continues to be a challenging and necessary endeavor. Such efforts are vital for informing future nuclear fuel cycle technologies, including applications in nuclear waste separations and environmental remediation, both of which require the ability to control actinide bonding and complexation under a variety of conditions and media. We are interested in exploring the non-aqueous chemistry of neptunium (Np) and plutonium (Pu) with an emphasis on elucidating electronic, bonding, and structural properties of complexes that exhibit metal-ligand multiple bonds. Specifically, we have used previously reported uranium (U) chemistry to guide synthetic efforts with the transuranic elements, with the aim of discovering trends, similarities, and differences in bonding and redox behavior across the 5f series.

«« Uranium is the heaviest element in the periodic table that is considered to naturally occur and be found in the environment. All the heavier elements known as the **transuranic elements** *are radioactively unstable to varying degrees, having been first discovered in the laboratory (although Np and Pu have since been found in nature in small quantities).*

Primarily due to their availability, and relatively low specific-activity, it is not surprising the most studied actinides are thorium (Th) and uranium—their chemistry can be performed easily and safely in academic laboratories with minimal radiological safety infrastructure. Consequently, increased efforts over the last several decades have resulted in a reimaging of contemporary knowledge of Th/U reactivity under a variety of experimental conditions, including the burgeoning field of anaerobic, non-aqueous molecular chemistry. In contrast, research involving high specific-activity transuranic isotopes (e.g., Np, Pu—the first two of the transuranic elements, see Fig. 1 below) requires specialized radiological facilities and, historically, has largely focused on complexes that are stable to air and/or water. Expanding the scope of this research to anaerobic, non-aqueous environments opens a wide range of possibilities in terms of bonding, oxidation states, and complexation studies. The knowledge gap between Th/U chemistry and that of the transuranics cannot be overstated (Fig. 2), especially considering it is the transuranic region of the actinide series that poses far greater challenges than Th/U regarding handling and long-term storage of nuclear materials.

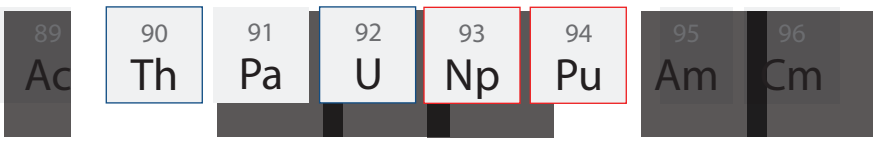

Figure 1. The early actinide element series.

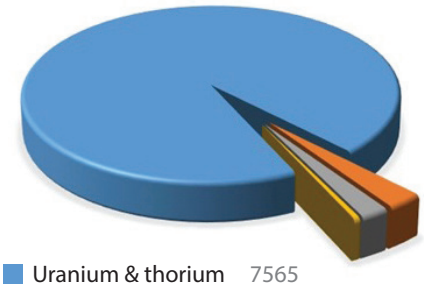

Figure 2. The number of Th and U complexes determined by X-ray structure methods dominate actinide chemistry (data source: Cambridge Crystallographic Data Centre, December 2018). This metric is a valuable gauge for measuring our knowledge of molecular metal complexes because X-ray methods now lead the way for characterizing these type of species.

»» *The gradual decrease in the ionic radii with the increase in atomic number is often called the* **actinide contraction**.

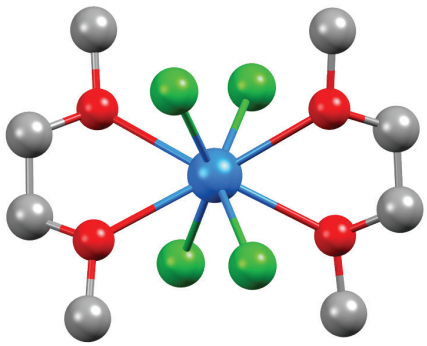

Figure 3. Solid-state molecular structure of $PuCl_4(DME)_2$. Hydrogen atoms are removed for clarity. Note, the neptunium analog is isostructural. [Pu = blue, O = red, Cl = green, C = gray]

Approach

It is generally accepted that as one traverses the 5f series, the elements become more lanthanide-like; in other words, actinides, especially those beyond Pu, exist primarily in the +3 oxidation state and exhibit predominantly ionic interactions (i.e., with minimal covalent bonding). This is attributed to the "actinide contraction" and the smaller ion size (or more accurately, the higher effective nuclear charge) with increasing atomic number. Recent advances in non-aqueous Th/U speciation have demonstrated a very broad range of coordination motifs, oxidation states, metal-ligand multiple bonds, and reactivity modes. Multiple bonds, in particular, are attractive targets to extend into the transuranic elements because they contain an inherent degree of covalent bonding character (overlap of metal and ligand based orbitals), and offer the opportunity to elucidate how these covalent bonding interactions change as a function of orbital radial extent, energy, and changing oxidation state stability across the actinide series. We have therefore targeted Np/Pu complexes that exhibit metal-ligand multiple bonding moieties in order to investigate how the 5f and 6d orbitals engage in covalent interactions compared to the analogous U species.

Preparing new anhydrous transuranic precursors

In order to extend non-aqueous Th/U coordination chemistry to Np/Pu, it is critical to first develop a similar 'tool-set' of starting materials. Np/Pu synthetic chemistry can be hindered by a lack of suitable anhydrous transuranic precursors, in particular precursors which are accessible using low-hazard procedures (avoiding high temperatures, reactive/toxic gases, etc.) and isolated in the desired oxidation states. For our purposes, ideal targets include Np/Pu starting materials that are neutral, soluble in a wide range of organic solvents, and exhibit either the +3 or +4 oxidation state. Although convenient access routes to Pu(III) halide-solvento species through oxidation of Pu metal are known, difficulties have been reported oxidizing the metal to Pu(IV) under similar conditions—for example, binary $PuCl_4$ has not been reported to be isolable. For Np, meanwhile, this chemistry is particularly challenging because the metallic form is scarce and therefore the oxidative pathways typically used to achieve the +3 oxidation state for U and Pu are not practical for Np. Aqueous stock solutions of Np(IV) are available, however, and given that both Th and U are known to form neutral, organic-soluble solvento adducts in the +4 oxidation state, an initial goal was therefore to replicate this for Np(IV) and Pu(IV).

The target molecules were successfully derived from readily available Np(IV) or Pu(IV) aqueous acidic stock solutions which, upon workup, resulted in the isolation of the transuranic solvento adducts, $AnCl_4(DME)_2$ (An = Np, Pu; DME = 1,2-dimethoxyethane). Both complexes were structurally characterized by X-ray crystallography (Fig. 3), and like their Th/U counterparts, they are soluble in organic solvents (e.g., DME, THF), exhibit readily assignable spectroscopic signatures, and are stable for use in a variety of ligand exchange reactions. This work demonstrates the power of donor solvent molecules to stabilize molecular species—we have shown that $PuCl_4(DME)_2$ is stable, whereas unsolvated $PuCl_4$ has not been isolated to date.

Both solvento species are valuable additions to the synthetic toolkit of neutral transuranic starting materials suitable for non-aqueous chemistry—since this work, Bart, Gaunt, and coworkers at Los Alamos National Laboratory (LANL) have recently demonstrated that $NpCl_4(DME)_2$ allows access to a well-defined Np(III) precursor.

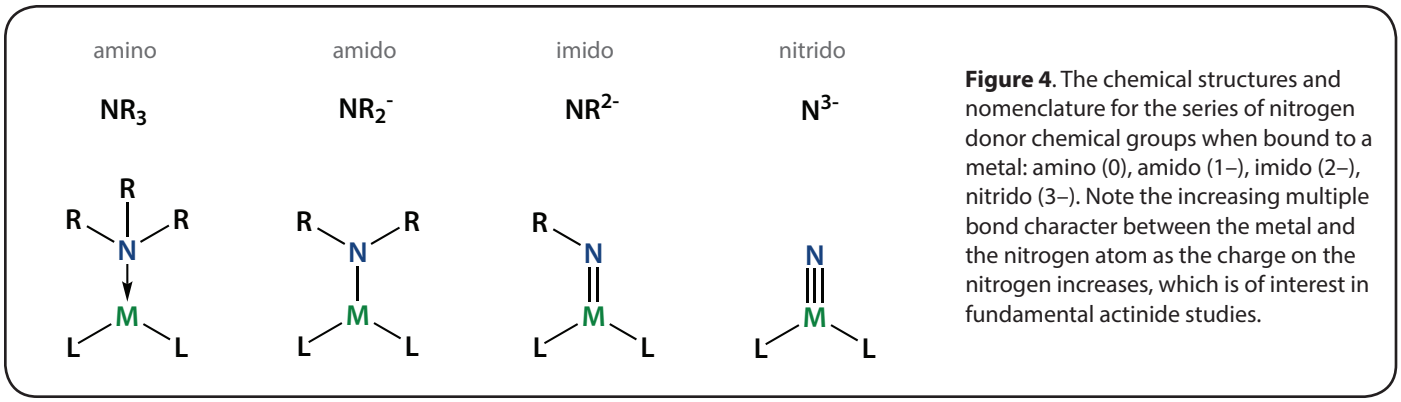

Figure 4. The chemical structures and nomenclature for the series of nitrogen donor chemical groups when bound to a metal: amino (0), amido (1–), imido (2–), nitrido (3–). Note the increasing multiple bond character between the metal and the nitrogen atom as the charge on the nitrogen increases, which is of interest in fundamental actinide studies.

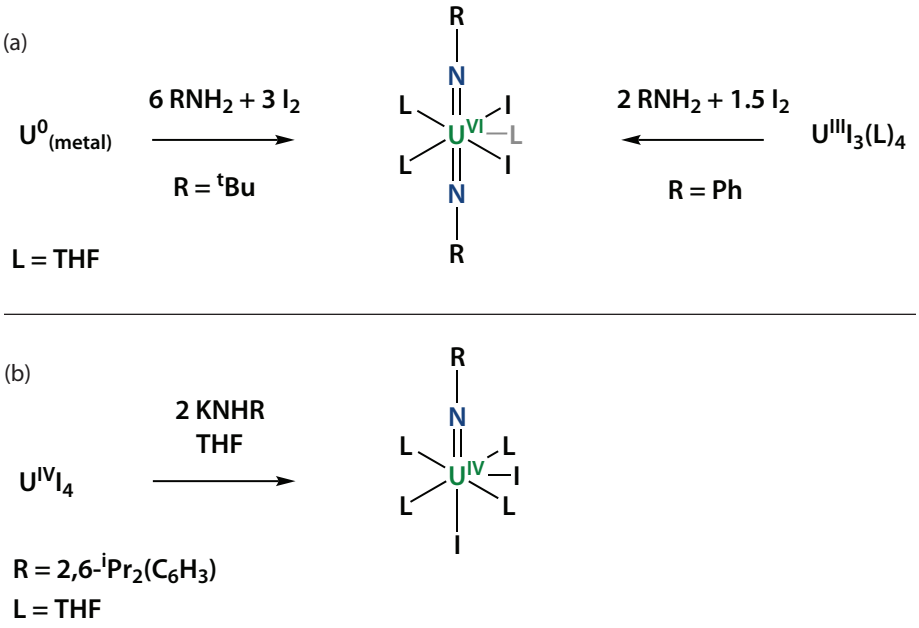

Figure 5. Previous work from the Boncella group showing the synthesis of **(a)** uranium(VI) bis-imido species from 2005 and **(b)** uranium(IV) mono-imido complexes from 2011. Note that iodine (I_2) acts as an oxidant in the bis-imido reactions, whereas there is no oxidant and no oxidation state change in the synthesis of the mono-imido species.

U imido complexes

To increase the probability of successful ligand exchange reactions in anhydrous transuranic chemistry, we again looked to known Th/U reactivity as a model. In 2005, Boncella and coworkers at LANL made a breakthrough in U-ligand multiple-bond chemistry with the isolation of two landmark uranyl (UO_2^{2+}) analogs, which contain two trans-imido groups (=NR, where R is a hydrocarbon—see Fig. 4 for details of the nomenclature of metal-bound nitrogen groups) in the place of oxo (=O). This type of bonding is ideal for studying covalency—an important concept in actinide chemistry, see article by Su on p11—as it allows one to probe the role and extent of valence 5f/6d orbital participation in metal-ligand bonding.

These compounds were synthesized in an oxidation reaction using either U metal or U(III) halide starting materials, leading to the target U(VI) bis-imido products (Fig. 5a). In 2011, the same group reported the first U(IV) mono-imido complexes, which were derived from U(IV) precursors in non-redox reactions (Fig. 5b). A collaboration with Boncella using transuranic elements led to this work exploring how covalency and/or multiple-bonding (beyond the ubiquitous actinyl dioxo fragment) manifests itself across the actinide series.

«« The ***"trans-"*** *prefix used in a chemical context denotes a geometric configuration in which two groups are located diametrically opposite each other, with respect to the metal center.*

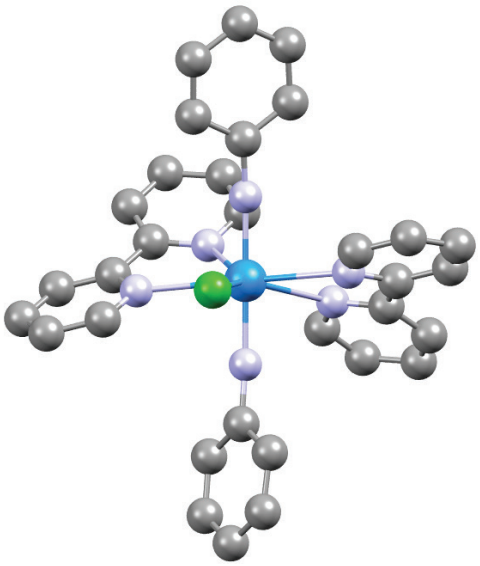

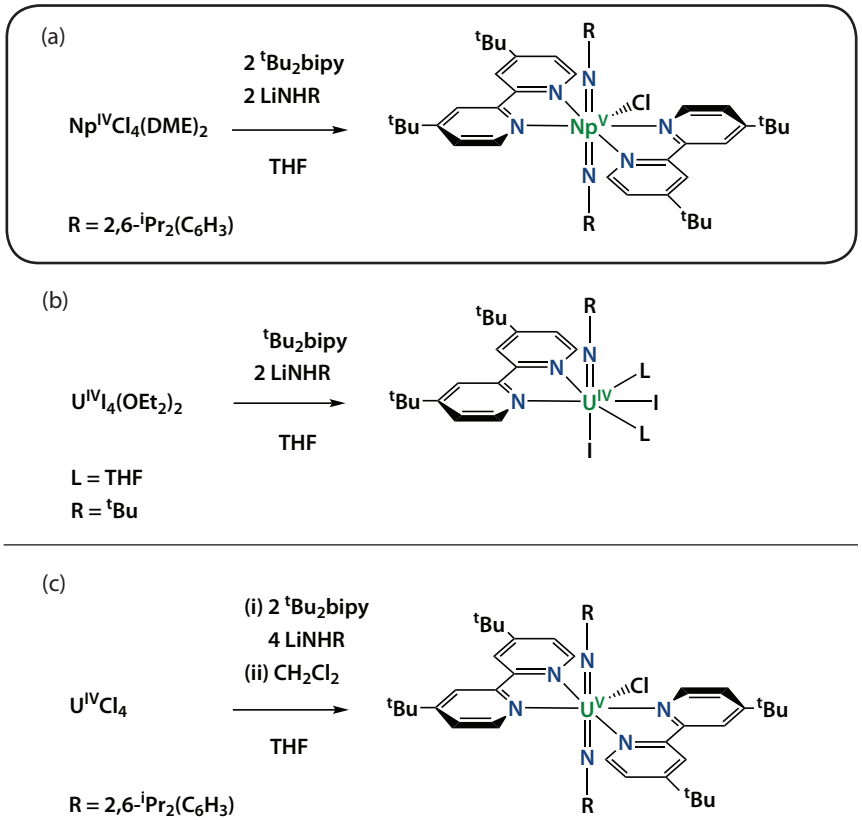

Figure 6. *Left*: Solid-state molecular structure of the novel Np(V) trans-bis-imido complex. H atoms, ^{i}Pr and ^{t}Bu groups, and co-crystallized non-bonding molecules are not shown, for clarity. Note the linear N–Np–N geometry. [Np = blue, N = light blue, Cl = green, C = gray]

Right: **(a)** Synthetic route to the Np(V) bis-imido complex. Note the oxidation state change from +4 to +5 without the use of an additional oxidant; **(b)** The same reaction conditions with U yield a mono-imido species, with no oxidation state change (Boncella group, 2011); **(c)** In order to synthesize the U(V) bis-imido analog, an additional oxidant must be used (CH_2Cl_2), as shown in work by the Boncella group in 2012.

Failed attempts to synthesize a Pu imido complex

Previous efforts to obtain a 'Pu=NR' moiety by mimicking the original methods reported for the U-imido chemistry unfortunately proved unsuccessful. This was likely due to the difficulty in achieving oxidation states greater than +3 when oxidizing Pu metal under anaerobic and anhydrous conditions. Alternative synthetic pathways utilizing Pu(III) precursors gave similar results—namely, no observation of a Pu-imido species in the +4, +5, or +6 oxidation states (i.e., the states commonly found in the U-imido analogs). The observed differences in the redox stability of U relative to Pu clearly demonstrate the need to study transuranic molecular chemistry in its own right, as extensions of one actinide's chemistry to its periodic neighbors are not always predictable or straightforward (as opposed to the lanthanide 4f series, which have remarkably similar properties).

Synthesis of the first Np imido complex

Despite the apparent 'synthetic reluctance' of Pu to form bis-imido species in high oxidation states (+5 or +6) Np remained a more likely candidate. Np lies between U and Pu on the periodic table and thus, may exhibit more U-like redox chemistry, especially with regard to the stability of higher oxidation states under anaerobic and anhydrous conditions.

Unfortunately the lack of Np metal or other suitable starting materials (at the time of these studies) prevented us following the same oxidative synthetic route to the U(VI) bis-imido compounds reported in 2005 (Fig. 5a); however, our new $NpCl_4(DME)_2$ complex allowed us to explore routes to target Np(IV) imido functionalities. Specifically, addition of an amide and a bipyridyl coligand to this in tetrahydrofuran (THF) afforded the linear Np(V) trans-bis-imido complex, which was structurally characterized by X-ray crystallography (Fig. 6). This is the first characterized example of a transuranic imido species.

Actinyl Ions

The actinyl ions, AnO_2^{n+}, consist of a linear dioxo fragment in a so-called "trans-" configuration (i.e. located opposite each other from the metal center), and exhibit short An-O bond lengths indicative of multiple bonding. The fragment is largely unreactive due to these incredibly strong bonds. Ligands in the equatorial plane are relatively labile in contrast, leading to a wealth of coordination chemistry.

Due to their ubiquitous nature under aqueous conditions, the actinyl ions are arguably the most technologically important and environmentally relevant fragment in actinide chemistry.

The imido (=NR) analogs so-far discovered are unstable under equivalent aqueous conditions, but still provide a valuable window into the mysteries of actinide molecular bonding.

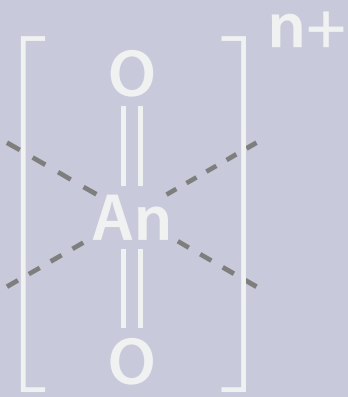

Surprisingly, we obtained a bis-imido species, despite the same reaction conditions for U chemistry giving a U(IV) mono-imido (Fig. 6b); furthermore, oxidation of the Np center from +4 to +5 was observed. This unprecedented Np bis-imido complex is structurally analogous to its U(V) bis-imido counterpart (prepared by Boncella under different reaction conditions, see Fig. 6c), being seven-coordinate in a distorted pentagonal bipyramidal geometry and exhibiting a linear $[RN=Np^{V}=NR]^{+}$ fragment (where R is a hydrocarbon) with Np-N bond distances comparable to those observed in the U(V) analog and indicative of significant multiple-bond character.

While the two actinide bis-imido complexes are structurally analogous, their preparative routes vary substantially, again highlighting the differences between U and Np reactivity. It is well documented in U chemistry that the employed stoichiometry will dictate the nature of the final U-imido product (i.e., the molar ratio of amide and pyridyl coligand, and presence or absence of halogenated solvent, will determine whether a mono- or bis-imido species is obtained). In contrast, regardless of the stoichiometry used, the Np(V) bis-imido complex is consistently isolated in reproducible, but low to moderate, crystalline yields (it should also be noted that ^{1}H NMR spectroscopy indicates that the leftover supernatant likely contains a complex equilibria of multiple Np species, similar to that found with U, explaining the low isolated Np(V)-bis-imido yields).

Bonding analysis: Comparison of U and Np bis-imido species

The isolation of this unprecedented Np(V) bis-imido species allowed a unique opportunity to elucidate its electronic structure via density functional theory (DFT), which could be based on experimental coordinates, and compare it with the previously reported U analog. The aim of the analysis was to gain insight into the extent of valence 5f/6d orbital participation in the 'An=NR' moiety and how covalency and/or multiple-bonding is changed as the actinide series is traversed. To reduce computational workload and promote convergence, slightly modified structures of the actinide-imido complexes were modeled and assessed. Importantly, the model systems exhibit theoretical structural parameters similar to those observed for the experimentally derived structures, thus providing confidence to any conclusions drawn from the model systems regarding the electronic structure of experimentally isolated complexes.

The DFT calculations (carried out by our collaborator, Enrique Batista, at LANL) demonstrated that there is appreciable metal-ligand orbital mixing in the actinide-imido functionality where the actinide 5f/6d orbitals and the nitrogen 2p orbitals exhibit significant orbital overlap. According to natural bond orbital analysis, the bonding orbitals are 24% metal-based in the U imido model and 30% metal-based in the Np imido model. Of this, the contribution from the 5f and 6d orbitals was similarly split in roughly a 55:45 and 60:40 ratio for the U and Np imido models, respectively. Overall, any observed differences between the two models is small, indicating their electronic structures are similar to one another. The analysis suggests that the valence 5f and 6d orbitals are indeed able to readily engage in metal-ligand multiple bond formation, alluding to the possibility that only the surface has been scratched and many more such bonding motifs are yet to be discovered for Np, and perhaps even Pu in the future. The observed differences in reactivity in our studies meanwhile likely stem from disparities in redox potentials between U, Np, and Pu.

Summary

Recent advances in transuranic molecular chemistry continue to demonstrate the need for well-designed and systematic studies to understand their unique speciation, oxidation state stability, and reactivity. While Th/U and lanthanide chemistry is a sound foundation from which to initiate transuranic reactivity studies, it is clear that the chemistry of Np and Pu can deviate significantly. Focusing on the key driving forces in non-aqueous transuranic speciation will allow us to close the knowledge gap that remains across the actinides and gain valuable insight into the trends and differences within the series regarding bonding, electronic structure, and reactivity.

Acknowledgments

The author thanks the G. T. Seaborg Institute at LANL for postdoctoral fellowship support, and the U. S. Department of Energy, Office of Science (Early Career Research program and the Basic Energy Sciences, Heavy Element Chemistry program) for funding this work. JLB also gratefully acknowledges the work of her co-workers in this collaborative project: Andrew J. Gaunt (mentor), James M. Boncella (U work), Enrique R. Batista (theoretical calculations and analysis), Sean Reilly (aqueous transuranic work), Brian L. Scott (crystallography), and Neil C. Tomson (U work).

Further reading:

1. *S. D. Reilly, J. L. Brown, B. L. Scott, and A. J. Gaunt, "Synthesis and Characterization of $NpCl_4(DME)_2$ and $PuCl_4(DME)_2$ Neutral Transuranic Starting Materials," Dalton Trans., 2014, 43, 1498.*
2. *J. L. Brown, E. R. Batista, J. M. Boncella, A. J. Gaunt, S. D. Reilly, B. L. Scott, and N. C. Tomson, "A Linear trans-Bis(imido) Neptunium(V) Actinyl Analog: $NpV(NDipp)_2(^tBu_2bipy)_2Cl$ (Dipp = 2,6-^{i}Pr$_2$C$_6$H$_3$)," J. Am. Chem. Soc., 2015, 137, 9583.*
3. *T. W. Hayton, J. M. Boncella, B. L. Scott, P. D. Palmer, E. R. Batista, and P. J. Hay, "Synthesis of Imido Analogs of the Uranyl Ion," Science, 2005, 310, 1941.*
4. *R. E. Jilek, L. P. Spencer, R. A. Lewis, B. L. Scott, T. W. Hayton, and J. M. Boncella, "A Direct Route to Bis(imido)uranium(V) Halides via Metathesis of Uranium Tetrachloride," J. Am. Chem. Soc., 2012, 134, 9876.*
5. *R. E. Jilek, L. P. Spencer, D. L. Kuiper, B. L. Scott, U. J. Williams, J. M. Kikkawa, E. J. Schelter, and J. M. Boncella, "A General and Modular Synthesis of Monoimidouranium(IV) Dihalides," Inorg. Chem., 2011, 50, 4235.*
6. *A. J. Gaunt, S. D. Reilly, A. E. Enriquez, T. W. Hayton, J. M. Boncella, B. L. Scott, and M. P. Neu, "Low-Valent Molecular Plutonium Halide Complexes", Inorg. Chem., 2008, 47, 8412–8419.*
7. *S. A. Pattenaude, N. H. Anderson, S. C. Bart, A. J. Gaunt and B. L. Scott, "Non-aqueous neptunium and plutonium redox behaviour in THF – access to a rare Np(III) synthetic precursor", Chem. Commun., 2018, 54, 6113.*

Toward High-Purity Actinide Nitrides: Uranium and Thorium Complexes with Nitrogen-Rich Tetrazolate Ligands

Kevin Browne

Kevin Browne was a Seaborg Institute Postdoctoral Research Fellow from April 2014 to March 2016 under the mentorship of Jacqueline Veauthier, Jaqueline Kiplinger, and Andrew Nelson, studying actinide coordination complexes with high-nitrogen content. He is now a Research Scientist at the Center for Naval Analyses Corporation in Arlington, VA.

At Los Alamos National Laboratory (LANL), actinide science relevant to energy and weapons applications has historically gone hand-in-hand with a firm understanding of the fundamental theoretical and experimental aspects of actinide properties. The road to "application-ready" uses for actinides has been paved with discoveries that have yielded key insights into actinide material properties, separation schemes, chemical reactivity, and electronic structure, to name just a few. In the work presented here, I explore actinide chemical reactivity from the standpoint of coordination chemistry and show its potential application for producing nuclear fuel.

My research goal was to investigate a new way to make thorium and uranium nitrides from well-defined small molecule precursors. Nitrides are the least utilized forms of fuel in nuclear power plants due to their challenging production methods—oxides and metallic thorium and uranium are more common fuels. The current synthetic method for making thorium or uranium nitrides is through a process known as carbothermic reduction and nitridation (CTR-N), shown in equations 1 and 2 below. While effective, this process is complex, and it is difficult to achieve large-scale, high-purity thorium and uranium nitrides in this manner.

(1) $3UO_2 + 6C \xrightarrow{>1200\ ^\circ C} 2UC + UO_2 + 4CO$

(2) $4UC + 2UO_2 + 3\ N_2 \xrightarrow{1800\ ^\circ C} 6UN + 4CO$

Approach

The methodology that I employed involves coordinating thorium or uranium precursors with ligands that contain a high percentage of nitrogen to yield coordination compounds (Fig. 1). Our goal is to ultimately perform thermolytic oxidation experiments in which the material is rapidly thermolyzed to yield uranium or thorium nitride. This energetic phenomenon could be expected in principle because the nitrogen-rich component of the sample may decompose to produce thermodynamically stable actinide nitrides following electron transfer, molecular rearrangement, and energetically favorable loss of N_2. There is precedent for nitrogen-rich ligands to react with transition metals upon laser-initiated ignition, but actinide reactivity has not been explored (safety first—nitrogen-rich molecules are potentially explosive, and we always assume that we've synthesized an energetic material until proven otherwise, therefore begin with small-scale syntheses and sensitivity-testing prior to scale-ups). Before this hypothesis could be tested, work was undertaken to better understand the bonding in the thorium and uranium precursor molecules with nitrogen-rich ligands.

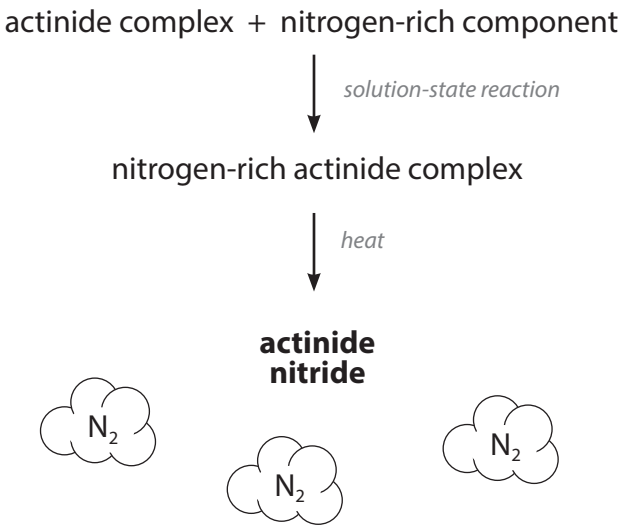

Figure 1. Simplified overview of the synthetic pathway towards actinide nitrides via thermal decomposition of nitrogen-rich complexes. The key step here is the thermodynamically favorable loss of N_2, which in principle yields very stable actinide nitride. The research described in this work focuses on the first step of this scheme.

Actinide tetrazole complexes

During this work, I developed model compounds that allowed us to further analyze how thorium and uranium bind to nitrogen-rich molecules. Despite decades of research focused on thorium and uranium, surprisingly little is known about their interactions with high-nitrogen molecules. The most studied nitrogen-rich ligand in actinide complexes is the azide moiety (N_3^-), whose bonding motifs with uranium and thorium range from end-on monomers to polymeric bridging. Since azides were already well-represented among nitrogen-rich actinide complexes, I chose to expand the library of accessible nitrogen-rich ligands by focusing on tetrazolate ($C(R)N_4^-$, where R is a hydrocarbon group). The actinide model compounds were carefully designed to bridge the gap between known species and the ideal, high-nitrogen actinide nitride precursors—this stepwise approach to introducing the nitrogen-rich component allows us to use prior knowledge and make reasonable predictions about chemical reactivity.

Fig. 2 shows X-ray crystal structures of two such compounds. The supporting cyclopentadienyl co-ligands have been widely employed in research of the molecular chemistry of thorium and uranium, and their chemical reactivity and analytical signatures are well understood. As a consequence, changes to other parts of the molecule can be interpreted within the context of the core unit—for example, there is a wealth of published data regarding the electrochemical behavior of a family of uranium compounds that contains the same motif. Furthermore, cyclopentadienyl ligands offer synthetic convenience, with readily accessible precursors and high crystallinity (an essential characteristic for structural analysis of paramagnetic compounds).

Bonding analysis

Our goal was to synthesize complexes in which the nitrogen component is bound more closely to the actinide center, as this should assist a successful thermally-induced nitridation reaction. The influence of nitrogen-rich tetrazoles on the properties of the uranium complex can be understood in several ways for this molecule. One direct and informative method is using cyclic voltammetry, which is an electrochemical measurement that uses a potentiostat to measure how easy or difficult it is to add/remove electrons to/from a compound. We found that it requires a potential of –1.88 V to add an electron to (i.e., reduce) the uranium compound shown in Fig. 2a. Another analytical technique that interrogates the nature of this

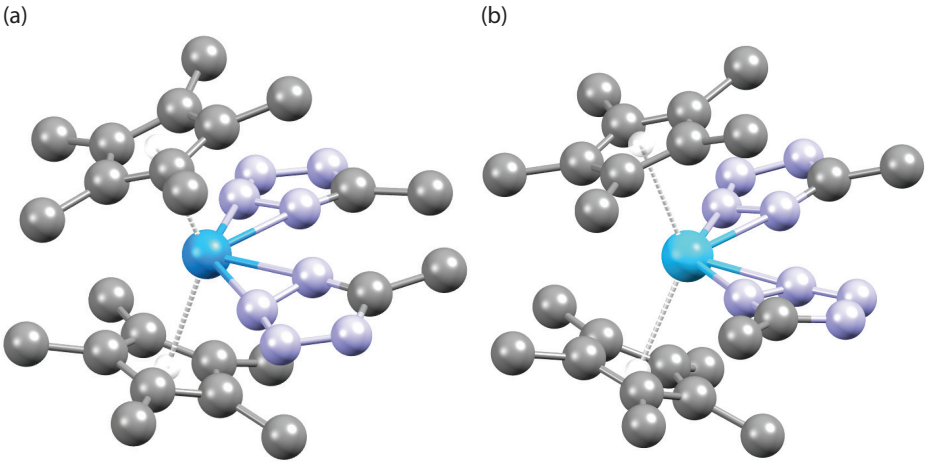

Figure 2. X-ray crystal structures of **(a)** uranium and **(b)** thorium compounds containing nitrogen-rich tetrazole ligands (H atoms omitted for clarity). At the center of the structures are the metal atoms (blue), and projected outwards towards the left of the structures are identical cyclopentadienyl ligands (carbon = gray). The nitrogen-rich component is visible on the right-hand side of the molecules—two five-membered tetrazole rings, each of which contains four nitrogen atoms (nitrogen = light blue). Note the subtle difference in orientation of one of the tetrazole ligands in the thorium structure in comparison to the uranium.

bonding is electronic spectroscopy, which probes the interaction of the compound with ultraviolet, visible, and near-infrared light. Based on our knowledge of how other organometallic uranium compounds absorb/transmit different wavelengths of light, it is possible to infer certain characteristics of the bond between uranium and tetrazole. Using both of these techniques, we can say with confidence that the chemical bond between uranium and tetrazole is a single bond (sigma bond), with negligible multiple-bond character.

While electrochemical and spectroscopic techniques provide useful insights into bonding and electronic structure, there are other analytical techniques for measuring the dynamic properties of these uranium and thorium tetrazole compounds. Two questions related to these properties were, "Does the tetrazole always stay bound in the same way to the actinide center, or can it change over time? And if so, what is the energy barrier to the change?" This line of questioning arose when we obtained the X-ray crystal structure of the thorium tetrazole complex (Fig. 2b), which is similar to the uranium analog but for one key difference—the orientation of the two tetrazole rings is opposite for the two compounds. Fig. 3 shows different possibilities for these orientations; while the uranium compound adopts configuration A, the thorium compound adopts configuration B. One possible implication of this observation is that the tetrazole rings interconvert between the two orientations while in solution form. We measured this interconversion using nuclear magnetic resonance (NMR) spectroscopy. By recording data at multiple temperatures, we found evidence that the tetrazole components of the thorium complex undergo interconversion between orientations A and B, and were able to determine that the energy difference between the two orientations in solution is between –6.98 and 1.63 kJ/mol at 298 K (at the 95% confidence interval).

Theoretical studies

Experimental data collected for the uranium and thorium tetrazolate complexes could allow us to make a generalization about the nature of the bond between metal and ligand in our new compounds. But to increase confidence in these conclusions, we pursued theoretical chemistry in parallel to our experiments. Our collaborators used density function theory (DFT) to reproduce our experimental results. DFT is a computational technique that uses software algorithms to derive equations that represent chemical bonding between atoms. Chemical bonds are most accurately described as the probability of electrons being shared by two atoms, and these probabilities can be visualized using representations like the one shown in Fig. 4.

«« **Nuclear Magnetic Resonance (NMR)** *obtains useful structural infor mation about a molecule by subjecting a pure sample of the compound to a strong magnetic field, and recording how the nuclei of the target atoms of the compounds (typically, hydrogen) respond to this field.*

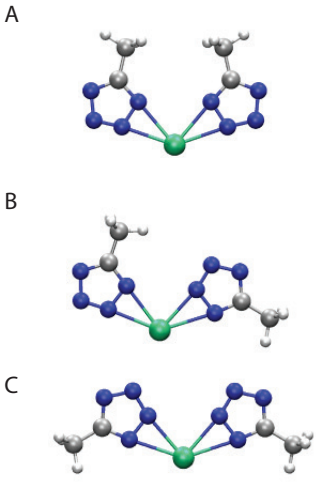

Figure 3. Different possible orientations of two tetrazole ligands coordinated to a central metal atom.

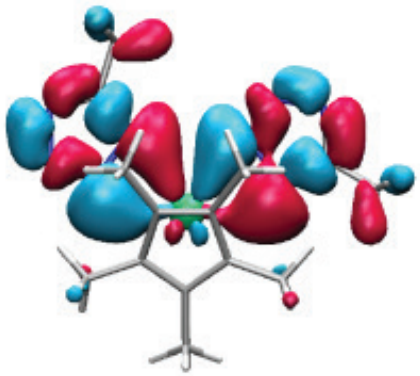

Figure 4. Selected molecular orbitals of the thorium tetrazole compound, calculated by density functional theory. The gray lines show the formal chemical bonds between atoms, while the blue and red curved surfaces represent molecular orbitals in which there is a certain probability for an electron to reside.

By capturing such minute, complex features computationally, it was then possible for our collaborators to reproduce many of the measurements we performed experimentally on the thorium and uranium tetrazole compounds, including cyclic voltammetry, electronic spectroscopy, and NMR. Not only does this work validate the experimental results, but it also helps to improve the theoretical approach, which is notoriously challenging for heavy-atom actinide species. Computational studies of the actinides feature many complex parameters, and the clear convergence of theory and experiment gives us confidence in employing DFT to make predictions for our future studies.

Summary

As we commence the next round of studies (in the lab and on the computer), we can move forward with confidence in our understanding of how one particular nitrogen-rich compound binds with thorium and uranium. While it is just one specific ligand employed here, we envision using this tetrazole core and derivatizing it to optimize its chemical properties. We have also validated our approach to synthesizing model compounds for comparing and contrasting our prior knowledge with new data, employing a common framework that allows for enough comparison among families of related compounds. While carbon-containing ligands are acceptable for model studies, they will likely create problematic impurities if pure nitrides are the only desired product. We hope to synthesize thorium and uranium compounds that contain only nitrogen-rich components—future work will aim to decrease the carbon content without sacrificing the convenient synthetic handle it provides. Although it is unlikely that this route will supersede the currently used industrial methods, our meticulous approach may give insight into the process of nitridation, which is difficult to study in a high temperature matrix.

Acknowledgments

For financial support of this work, we acknowledge the U.S. Department of Energy through the LANL LDRD Program, the LANL G.T. Seaborg Institute for Transactinium Science (PD Fellowship to Kevin P. Browne), and the Office of Basic Energy Sciences, Heavy Element Chemistry Program. This research used resources provided by the LANL Institutional Computing Program.

Models for Waste Compatibility: Actinide Catalysts and Amine Boranes

Karla A. Erickson

Karla Erickson was a Seaborg Institute Postdoctoral Research Fellow from November 2015 to October 2017, working under the mentorship of Jaqueline Kiplinger. Her research interests included actinide catalysts and their role as models for waste compatibility. She is currently a staff scientist in the Chemical Diagnostics and Engineering group (C-CDE).

Catalysts are molecules that mediate energetically challenging reactions an infinite number of times—ideally—without degrading. They play a pivotal role in modern industry and are responsible for, among many other applications, production of cheap, versatile plastics, the reduction of polluting gases from automobiles, and the synthesis of ammonia, which is key for synthetic fertilizers that promote high-yielding crops. Evolving priorities ultimately direct the focus of research programs, resulting in an intriguing interplay between science and society. In the hope of discovering more efficient or new types of catalysts, chemists study metal-centered molecules with high-carbon ("organic") frameworks. A seemingly infinite combination of transition metals and ligands are possible since the organic frameworks can be tailored to exhibit an array of electronic and geometric properties, which impart varying effects on the subsequent reactivity.

Studies of actinide catalysts are comparatively scarce and poorly developed. Regulatory barriers and overall public distaste have fueled a perception that there are no catalytic applications of actinide chemistry. However, uranium metal was originally found by Fritz Haber to be the most efficient catalyst studied in his eponymous nitrogen fixation process; this reaction is now used to provide half of the nitrogen in the world's food supply—needless to say, using a non-radioactive transition metal catalyst. Nonetheless, actinide materials continue to find extensive use, e.g., as power sources in nuclear fission and space exploration. Understanding their often unpredictable behavior, such as in aging nuclear waste, is a compelling motivation for further study. Modeling these behaviors and applications based only upon our knowledge of transition metal chemistry is virtually impossible due to the intrinsically unique properties of the actinides.

The actinide elements have f electrons, in f orbitals while transition metals utilize d electrons in differently-shaped d orbitals (see article by Su and explainer on p12). The orbitals are, roughly speaking, descriptors of the spatial extent that the electrons can populate, and have important ramifications in chemical bonding. Actinides, being heavier atoms, also have larger atomic radii, allowing for these metals to support uniquely bulky ligand frameworks and unusual intramolecular interactions. These qualities operating in concert provide new and exciting avenues to pursue in light of the contrasting chemistry actinides display compared with transition metals.

Actinide-catalyzed gas evolution studies

Coming from a background in transition metal catalysis, I became interested in studying the generation of gaseous products from actinide complexes, especially given events such as the unexpected emission of gases from nuclear waste storage tanks in Hanford, Washington, and a 2017 irradiation incident at Japan's Oarai

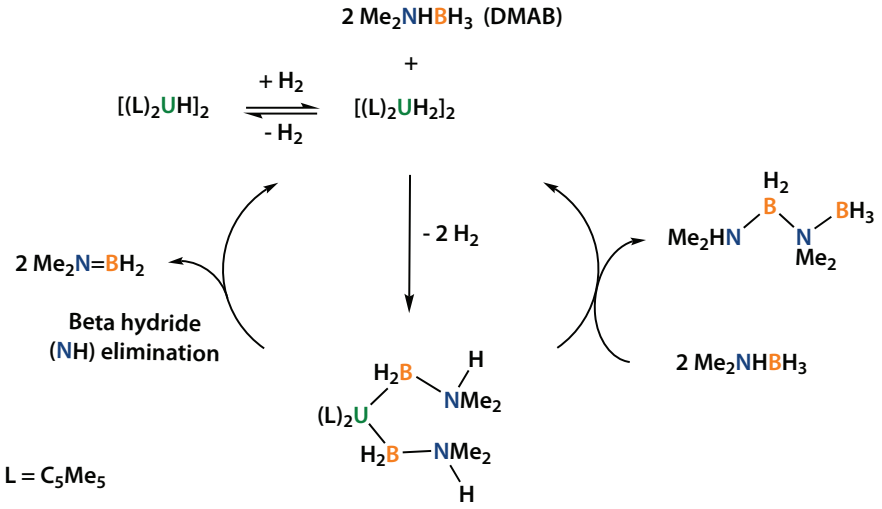

Figure 1. A proposed catalytic cycle for the dehydrogenation of dimethylamine borane, $Me_2NH{\cdot}BH_3$ (DMAB), includes β-hydride elimination steps to produce the active actinide hydride catalytic species.

Research and Development Center, caused by plutonium in direct contact with plastic (polyethylene), which generated hydrogen and other gases.

I began a proof-of-concept study focused on the generation of flammable hydrogen gas from amine borane substrates as a foray into understanding processes that may be pertinent to waste issues. My choice of substrate, amine boranes, $R_2HN{\cdot}BH_3$ (where R is a hydrocarbon) have both protic (H^+) amine and hydridic (H^-) borane hydrogen atoms and are poised for hydrogen gas elimination (dehydrogenation). They have also been proposed as possible hydrogen fuel storage materials. Therefore, this actinide-catalyzed gas evolution study simultaneously explores both energy storage and waste compatibility applications.

The dehydrogenation of amine boranes with transition metal elements has been extensively studied, affording over 1000 scientific papers and 50 literature reviews alone. No reports exist for actinide-based catalysts, indicating that these studies are timely and any unusual catalytic behavior should become immediately apparent. Using known dimethyl actinide complexes $(C_5Me_5)_2AnMe_2$ (An = Th, U; Me = CH_3, methyl) as precatalysts we have found H_2 gas is rapidly eliminated from a series of commercially available amine boranes, $Me_2NH{\cdot}BH_3$ (dimethylamine borane, DMAB), $^tBuNH_2{\cdot}BH_3$ (tert-butylamine borane, TBAB), and $NH_3{\cdot}BH_3$ (ammonia borane, AB). In these substrates we have varied the amine component and have uncovered an array of intriguing and fundamentally important characteristics, including unique catalyst activation steps and novel bonding motifs. Despite these differences, the overall steps to catalytically generate H_2 are satisfyingly consistent with each other.

»» The term **precatalyst** *describes a chemical species in the form which is added to a reaction mixture to perform catalysis. This strictly differentiates it from its true catalytic form, which can have a different molecular structure that has arisen from chemical reactions within the mixture.*

Catalysis results: Dimethylamine borane

Dehydrogenation of DMAB with $(C_5Me_5)_2AnMe_2$ occurs at room temperature, resulting in vigorous evolution of H_2 gas that bubbles from the reaction solution. We found that close to 500 molecules of DMAB are consumed over the course of six hours when mixed with one molecule of $(C_5Me_5)_2AnMe_2$. These metrics are superior to the majority of reported transition-metal systems; however, a handful of other reported catalysts are nearly three times faster utilizing a rhodium metal center and phosphine ligands.

Interestingly, the study of a 2:1 mixture of DMAB:$(C_5Me_5)_2AnMe_2$ shows that the methyl group of the actinide is not eliminated as methane (CH_4), which would

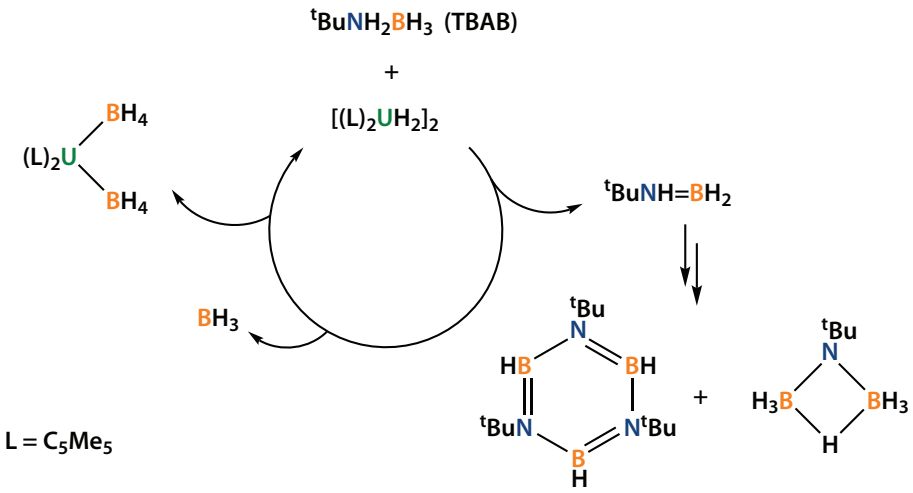

Figure 2. A general scheme showing key transformations in the dehydrogenation of tert-butylamine borane, $^{t}BuNH_2{\cdot}BH_3$ (TBAB). This dehydrogenation has fewer well-defined steps when compared to that for dimethylamine borane, $Me_2NH{\cdot}BH_3$ (DMAB). Nevertheless, β-hydride elimination and the formation of actinide hydrides are key unifying themes between these two systems.

be entropically favorable and is a reasonable first step ($CH_3^- + H^+ \rightarrow CH_4$). Instead, the actinide methyl group is transferred to the borane of $Me_2NH{\cdot}BH_3$, producing complexes such as $(C_5Me_5)_2An(BHMe{\cdot}NMe_2H)_2$, which are stable long enough in solution to be observed by nuclear magnetic resonance (NMR) spectroscopy. These complexes slowly eliminate $Me_2N{=}BHMe$, as observed by ^{11}B NMR spectroscopy. The "amino borane" products, $Me_2N{=}BHMe$ and $Me_2N{=}BH_2$, which were observed in catalytic reactions, are relevant to the mechanism and are indicative of β-hydride elimination from intermediates such as $(C_5Me_5)_2An(BHR{\cdot}NMe_2H)_2$ (Fig. 1). This is of fundamental importance, since β-hydride elimination has rarely been documented at actinide centers.

We propose that the H atom on the element β from the actinide (i.e., located two atoms away in the bonding chain; nitrogen, in this case) is intramolecularly abstracted by elimination of $Me_2N{=}BHR$. Upon abstraction of the N–H proton by the actinide center, a metal hydride complex such as $[(C_5Me_5)_2An(H)_2]_2$ could form, which we propose is the catalytically active species. In order to confirm this, these hydride complexes were independently synthesized and treated with catalytic (i.e., smaller) amounts of DMAB. The actinide hydride complexes behaved in a similar manner to the original dimethyl precatalyst $(C_5Me_5)_2AnMe_2$.

Tert-butylamine borane

Many similar themes are found in the chemistry of $(C_5Me_5)_2AnMe_2$ with TBAB, including transfer of the actinide-bound methyl groups to borane, β-hydride elimination, and the catalytic activity of actinide hydrides (Fig. 2). Additionally, we found that the actinide catalysts outperformed all previously reported catalysts for TBAB dehydrogenation, even though these metrics are lower than those observed for DMAB. Here, we only converted <30 molecules of TBAB to product (per molecule of catalyst). We attribute the challenges associated with TBAB dehydrogenation to the increased electronic donation of the tert-butyl group, which weakens the B–N bond and ultimately leads to B–N cleavage. Subsequent competing chemical processes, such as the formation of the aminodiborane $^{t}BuNHB_2H_5$, ensue. B–N cleavage chemistry is also detrimental to the catalyst. We showed that the proposed catalytically active actinide hydride complexes react with BH_3 (a product of B-N cleavage) and form the corresponding, known actinide borohydride complexes $(C_5Me_5)_2An(BH_4)_2$, which are not catalytically active, thus quench catalysis.

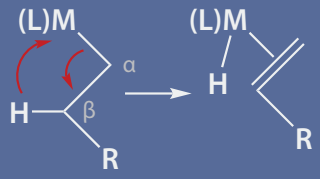

«« **β-hydride elimination** *is a reaction in which a group bound to a metal ion internally reacts to form the corresponding metal bonded hydride and an unsaturated bond. The "β" term derives from the location of the abstracted hydrogen—the β position is located two atoms away in the bonding chain. It can often be an important step in catalysis, forming a catalytically active hydride. On other occasions, it can hinder catalysis and represents a "dead end" chemical route. In these cases, chemists will often re-design their catalyst so that it does not bear reactive hydrogen atoms at the β position.*

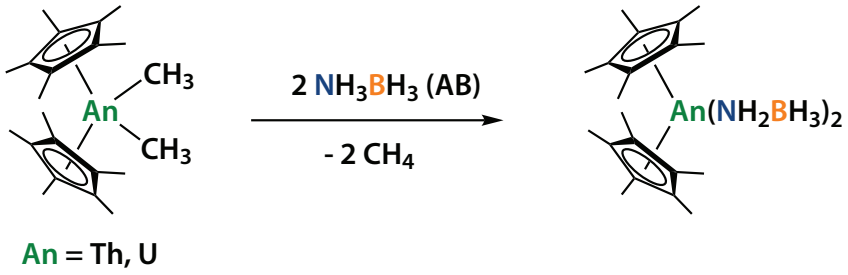

Figure 3. In ammonia borane (AB) reactions, the methyl groups are eliminated as methane, rather than transferred to borane, as observed in alkyl amine borane dehydrogenation.

Ammonia borane

The chemistry observed with AB is radically different. First, AB has limited solubility in common laboratory solvents, requiring in our case the use of the coordinating solvent tetrahydrofuran (THF), which can bind to the actinide center and block incoming substrate. We believe this is in part responsible for the poor, barely-catalytic metrics that are observed for AB dehydrogenation. Treatment of actinide complexes $(C_5Me_5)_2AnMe_2$ with two equivalents of AB in THF shows other dramatic differences. Whereas the actinide methyl group is transferred to the borane in reactions with DMAB and H_2 only forms under catalytic conditions (i.e., excess substrate), here, gas evolution occurs immediately, indicating that the actinide methyl group is instead eliminated as methane (CH_4), representing two opposed mechanisms. The resulting species $(C_5Me_5)_2An(NH_2{\cdot}BH_3)_2$ were observed by ^1H NMR spectroscopy (Fig. 3). The solid-state crystal lattice of $(C_5Me_5)_2Th(NH_2{\cdot}BH_3)_2$ was contaminated with molecular structures of inconsistently-oriented amidoborane molecules, which prevented the determination of a definitive solid-state structure. However, the uranium solid-state structure was successfully obtained using X-ray diffractometry and shows fascinating features, including two different interactions between borane (BH_3) and the uranium center. In one amidoborane $(NH_2{\cdot}BH_3)^-$ ligand, one borane hydride is oriented towards uranium, whereas in the second amidoborane ligand, two borane hydrides are oriented towards uranium.

Computational studies

A collaboration with computational chemists has helped us better understand these thorium and uranium amidoborane complexes. Geometry optimization calculations showed that the thorium complex $(C_5Me_5)_2Th(NH_2{\cdot}BH_3)_2$ has a different

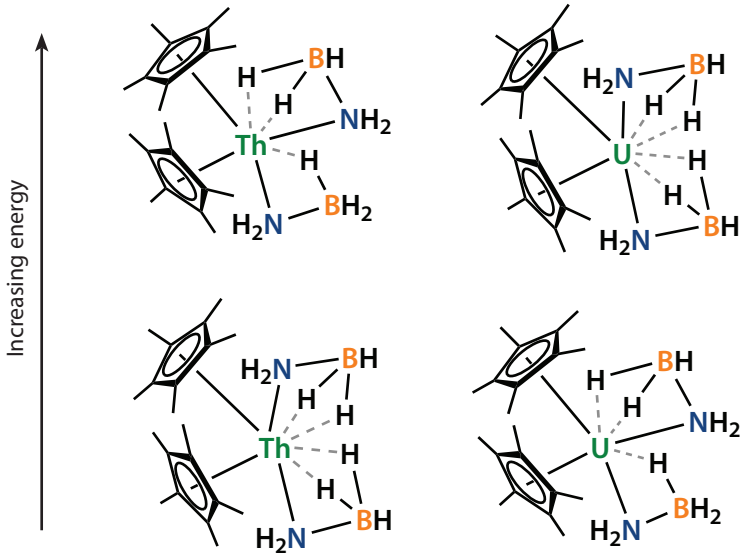

Figure 4. Multiple actinide isomers are formed upon coordination of the amidoborane ligand. These isomers reflect different orientations of the amidoborane ligand and different borane (BH_3) interactions with the metal center, resulting in unique structures.

structure in the solid state compared with the uranium complex (Fig. 4, lower panel). In the thorium complex, the amidoborane ligands are mirrored and both borane moieties orient to present two hydrides to thorium. However, a second thorium complex is also stable at room temperature, and features amidoborane ligands arranged analogously to the uranium structure (Fig. 4, upper panel). The energy difference between the two thorium structures (isomers) is very small, <1 kcal/mol. Interestingly, the uranium complex also features a second isomer, which is higher in energy than the two thorium isomers. The geometry of the second uranium isomer is analogous to the lowest energy thorium isomer. The energy differences between the uranium and thorium isomers explain why the lowest energy uranium isomer was isolated at low temperatures while thorium contained a mixture of bonding motifs.

Calculations showed that the borane hydrides, which are oriented towards the metal, donate electron density to the actinide to form weak "agostic" interactions. Agostic interactions are informative because they represent a structural snapshot in the process towards bond cleavage. In $(C_5Me_5)_2An(NH_2{\cdot}BH_3)_2$, the β-atom participates in the agostic interaction, which has not been previously reported for actinide complexes. Nevertheless, the overall picture is consistent: we observe β-agostic interactions in the actinide complexes that show the slowest catalysis with AB, which are proposed intermediates in the β-hydride elimination steps that rapidly occur in the dehydrogenation of DMAB and TBAB.

Summary

The actinide complexes $(C_5Me_5)_2AnMe_2$ (An = U, Th) were found to be highly active dehydrogenation catalysts for DMAB and TBAB. The reactions proceed through a β-hydride elimination mechanism, which has only been previously reported in photochemical reactions with actinide hydrocarbon systems. Destabilization of the B–N bond in TBAB results in competing pathways and slower catalytic metrics than those for DMAB. The actinide hydride complexes $[(C_5Me_5)_2An(H)_2]_2$ trap borane (BH_3), a product of B-N cleavage, which affords the catalytically-inactive borohydride species $(C_5Me_5)_2An(BH_4)_2$. The actinide catalysts react with AB to afford fascinating complexes that reveal fundamentally important interactions between the borane and actinide.

This work explores fundamental actinide chemistry which is part of our growing efforts to understand and model more complex and application-based scenarios. Future plans are being developed to explore actinide complexes with environmentally-pertinent molecules to continue our efforts in real world situations.

Further reading:

1. *A. Staubitz, A. P. M. Robertson, and I. Manners, "Ammonia-borane and related compounds as dihydrogen sources", Chem. Rev., 2010, 110, 4079.*
2. *A. Staubitz, A. P. M. Robertson, M. E. Sloan, and I. Manners, "Amine– and phosphine–borane adducts: New interest in old molecules", Chem. Rev., 2010, 110, 4023.*
3. *K. A. Erickson, and J. L. Kiplinger, "Catalytic dehydrogenation of dimethylamine borane by highly active thorium and uranium metallocene complexes", ACS Catalysis, 2017, 7, 4276.*
4. *A. Rossin, and M. Peruzzini, "Ammonia–borane and amine–borane dehydrogenation mediated by complex metal hydrides", Chem. Rev., 2016, 116, 8848.*
5. *K. A. Erickson, B. L. Scott, and J. L. Kiplinger, "$Ca(BH_4)_2$ as a simple tool for the preparation of thorium and uranium metallocene borohydride complexes: First synthesis and crystal structure of $(C_5Me_5)_2Th(\eta^3\text{-}H_3BH)_2$", Inorg. Chem. Commun., 2017, 77, 44.*
6. *M. Brookhart, M. L. H. Green, and G. Parkin, "Agostic interactions in transition metal compounds", Proc. Natl. Acad. Sci., 2007, 104, 6908.*

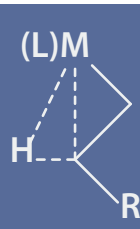

«« **Agostic bonding**, *derived from the Greek word meaning "to hold close to oneself", is a type of bonding seen in coordination compounds in which a terminal bond on a ligand (often a C-H) donates electron density to an electron-deficient metal center.*

Acknowledgments

K.A.E. was supported through the Glenn T. Seaborg Institute for the duration of this project. Other contributors include Stephen K. Cope, Brian L. Scott, David E. Morris, Pavel Dub and Jaqueline L. Kiplinger. Naveen K. Dandu and Samuel O. Odoh (University of Nevada, Reno) are acknowledged for their computational work in support of this project.

Sarah C. Hernandez

Sarah C. Hernandez received her PhD from the University of Texas at Arlington in Physics and started a postdoctoral appointment at Los Alamos National Laboratory immediately afterwards in March of 2015. She was a Seaborg Institute Postdoctoral Research Fellow from May 2015 to August of 2016, working under the mentorship of Thomas J. Venhaus. Her studies include the oxidation and corrosion of plutonium and aging of plutonium using density functional theory methods. She is currently a staff scientist in the Materials Science and Technology Division, Nuclear Materials Science Group (MST-16).

New Surface Science Instrumentation for Understanding the Reactivity of Plutonium

The Plutonium Surface Science Laboratory (PuSSL) located in the Target Fabrication Facility (TFF) at Los Alamos National Laboratory (LANL) has allowed studies of plutonium (Pu) surfaces in a laboratory setting. New scientists can study Pu more easily at this facility because it does not require all the extensive training needed to work in the plutonium facility (PF-4). The capability allows students and early career staff to obtain experience with surface science instrumentation that is fully configured for the study of radioactive materials.

Operations in the PuSSL have grown since its inception nearly 10 years ago with the help of many scientists, technologists, and technicians, in addition to operational and radiation protection support. The lab is equipped with a suite of instruments, including: polarization-modulated Fourier transform infrared reflection difference micro-spectroscopy (PM-IRRAS), X-ray photoelectron spectroscopy (XPS), ellipsometry, time-of-flight secondary ion mass spectrometry (ToF-SIMS, see Fig. 1), scanning tunneling microscopy (STM), and atomic force microscopy (AFM). In many cases, these surface analytical techniques have never been applied to Pu surfaces and are providing new insights into our understanding of Pu reactivity. Another unique feature of the PuSSL is the ability to transfer samples quickly between the various instruments. Due to the fact that Pu samples are radiologically toxic, samples must be contained at all times (i.e., no exposure to the lab environment)—to meet this requirement, samples are prepared in PF-4 and transferred to the TFF via a hand carry procedure.

The surface of Pu metal is highly reactive, and forms a mostly passivating oxide layer readily upon exposure to air. If the passivated layer is compromised it can further accelerate corrosion of the surface, forming particulates of Pu oxide which are detrimental to the environment and the health of the worker. Also, the nature of the oxide, i.e., a tetravalent (4+) versus trivalent (3+) oxidation state, can render it more susceptible to forming Pu hydrides, which proceeds via a pitting corrosion mechanism. Therefore it is imperative to fully understand the oxidation and corrosion mechanisms at the Pu metal and oxide surface, and how impurities that may exist on the surface can influence these mechanisms.

Introduction to time-of-flight secondary ion mass spectrometry

ToF-SIMS is a highly surface-specific analytical technique that provides an analysis of the outer 1–2 monolayers of the surface (<1 nanometer, nm). In contrast, XPS has an approximate probe depth of 5–9 nm (see box on following spread). ToF-SIMS can be sensitive to chemical impurities at parts-per-million (ppm) levels, and is one of the few surface science techniques that can detect hydrogen, which is useful in the case of detecting metal hydride species. The ToF-SIMS technique directs a pulse of primary ions onto the surface of interest. These energetic primary ions from the beam are implanted into the surface and, due to the reflective energy

ToF-SIMS instrumentation

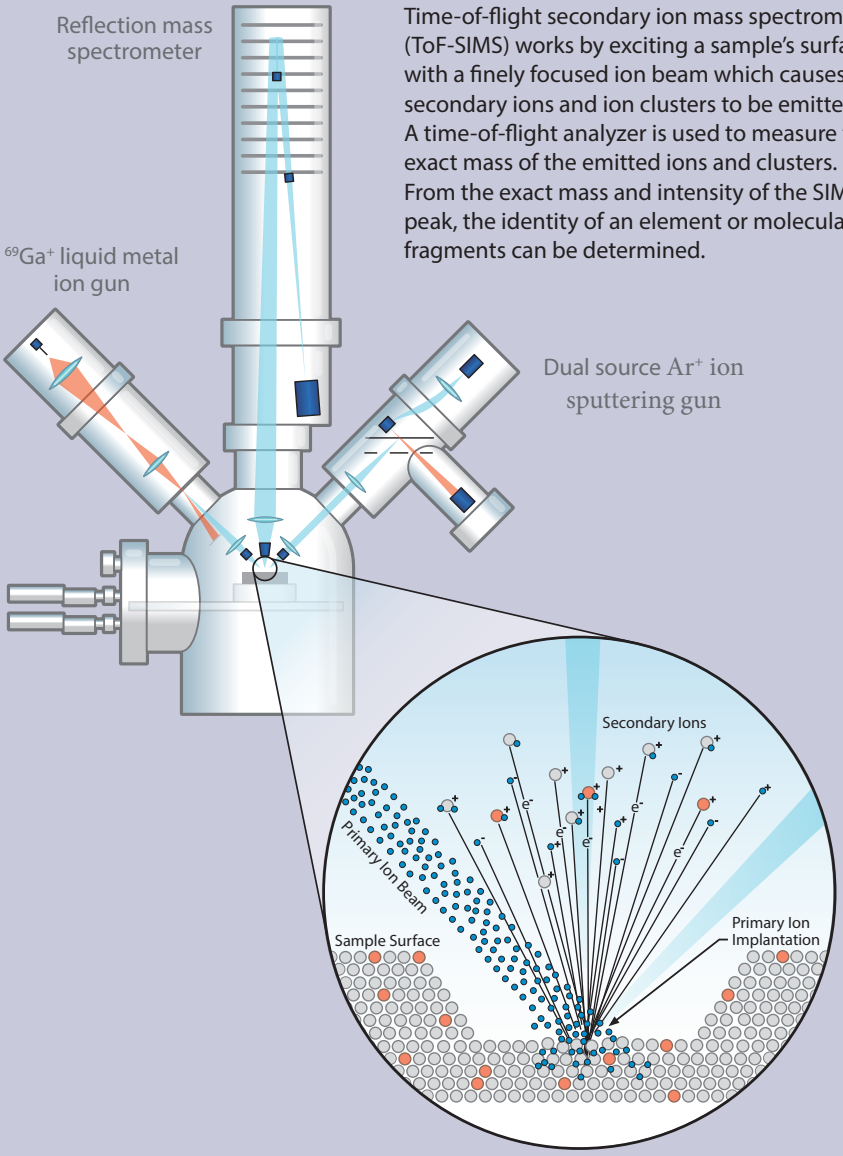

Time-of-flight secondary ion mass spectrometry (ToF-SIMS) works by exciting a sample's surface with a finely focused ion beam which causes secondary ions and ion clusters to be emitted. A time-of-flight analyzer is used to measure the exact mass of the emitted ions and clusters. From the exact mass and intensity of the SIMS peak, the identity of an element or molecular fragments can be determined.

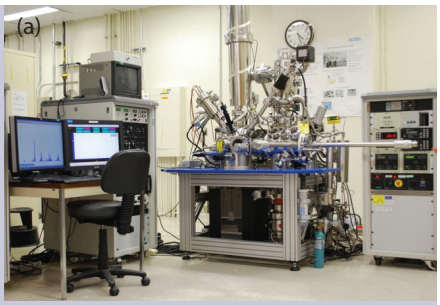

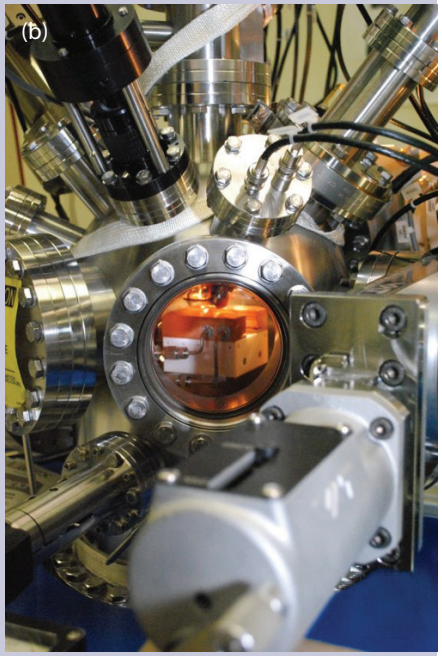

Figure 1. **(a)** The Kore ToF-SIMS instrument located in the Target Fabrication Facility (TFF). **(b)** View inside the sample analysis chamber of the ToF-SIMS instrument.

from the implantation, a small fraction of the surface atoms are ejected in the form of charged ions, molecules, and clusters with just a few eV of energy. The ions are then accelerated into a flight tube to a given energy and their velocity can be determined by measuring the time it takes for the ion to travel the distance to the detector. For a given quantity of kinetic energy, lighter ions will travel faster, reaching the detector at a time determined by their mass, hence "time-of-flight" spectrometry. The mass is then calculated via the simple kinetic energy formula from classical mechanics (kinetic energy = ½ mass × velocity^2).

Sputtering used to remove surface contaminates

The process for ion-induced secondary ion emission is complex, yielding varied ion fragments that are highly dependent upon surface oxidation state and impurity levels. These factors may yield unpredictable and often meaningless spectra from

Surface Analysis Depths

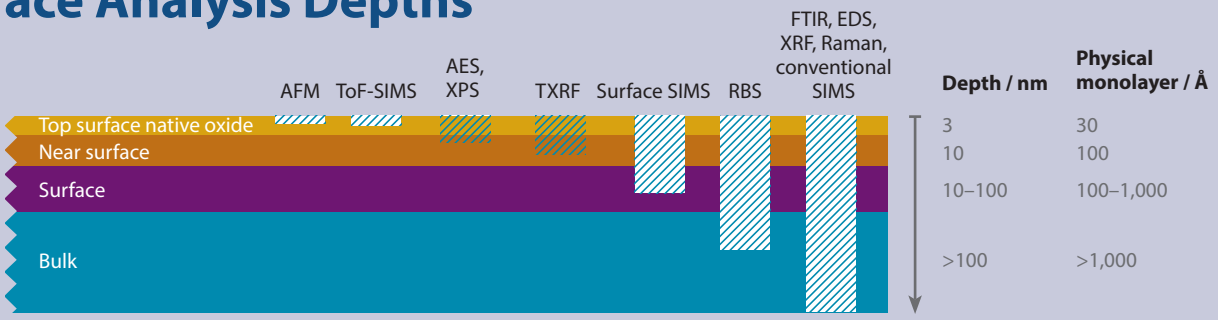

Each type of analytical instrumentation provides different information on the surface and probes varying depths of solid-state regimes, as shown above.

There are three types of mass analyzers for SIMS: sector field, quadrupole, and time-of-flight, and two types of modes for SIMS: dynamic and static. Dynamic SIMS is known to be a destructive technique as it will provide information on the bulk composition, whereas static SIMS aims to be a quasi-non-destructive technique in order to analyze the undisturbed topmost few monolayers of a surface.

Dynamic and static SIMS techniques are controlled by the density flux of the bombardment of the primary ions on the surface. By setting a low primary ion flux density, static SIMS causes negligible damage (>1%) to the surface, contrary to dynamic SIMS. For dynamic SIMS, sector field or quadrupole mass analyzers are used, whereas the time-of-flight mass analyzer is the standard and most efficient spectrometer for static SIMS. Thus, ToF-SIMS is a highly surface-sensitive analytical technique that combines both the SIMS technique with a time-of-flight mass analyzer.

Figure 2. Coupons of 7 at. % Ga-stabilized δ-Pu.

an "as-received" surface due to possible recombination of the secondary ions from surface preparation residue. To simplify the spectra, low-energy ion bombardment (sputtering) is used to reduce the level of contaminants that remain from surface preparation steps (cutting, polishing, and cleaning). Used more aggressively, the process can effectively remove the outer oxide layer itself, providing access to the oxide sub-layer and even bare Pu metal for a short time in ultra-high vacuum. The ToF-SIMS instrument located in the PuSSL uses a monoisotopic 69-gallium ($^{69}Ga^{+}$) liquid metal ion gun (LMIG) and also has an argon (Ar^{+}) ion sputtering gun in order to perform interlacing depth profiling (Fig. 1). An LMIG source heats the metal to a liquid to form a beam of ions that is focused towards the surface of the sample, and because Ga has a low melting temperature it is usually the preferred metal ion source. It should be noted that ToF-SIMS is highly sensitive to halogens, as they are highly electronegative and easily ionized, which will influence the yield intensity of the detected ion fragments. Thus, quantification of these surface contaminants is very difficult with ToF-SIMS (as with most mass spectrometry-based techniques), and techniques such as XPS and Auger electron spectroscopy (AES) are far more reliable to obtain quantitative results of the atomic percent level of these surface species.

ToF-SIMS analysis of the plutonium surface

Plutonium metal is highly reactive and immediately forms an oxide layer when exposed to air, as summarized by John M. Haschke et al. in "Surface and Corrosion Chemistry of Plutonium," published in Los Alamos Science No. 26, 2000. While XPS is powerful for detecting an oxide layer via valence states, the strength of ToF-SIMS is its ability to detect secondary ion fragments that provide clues as to how molecules are bound to the surface. Certain fragment patterns can indicate physisorption, dissociation, or chemisorption following gas exposures. Since ToF-SIMS is sensitive to isotopes, using isotopically labeled gases (e.g., $^{16}O_2$ versus $^{18}O_2$) for gas exposures, one

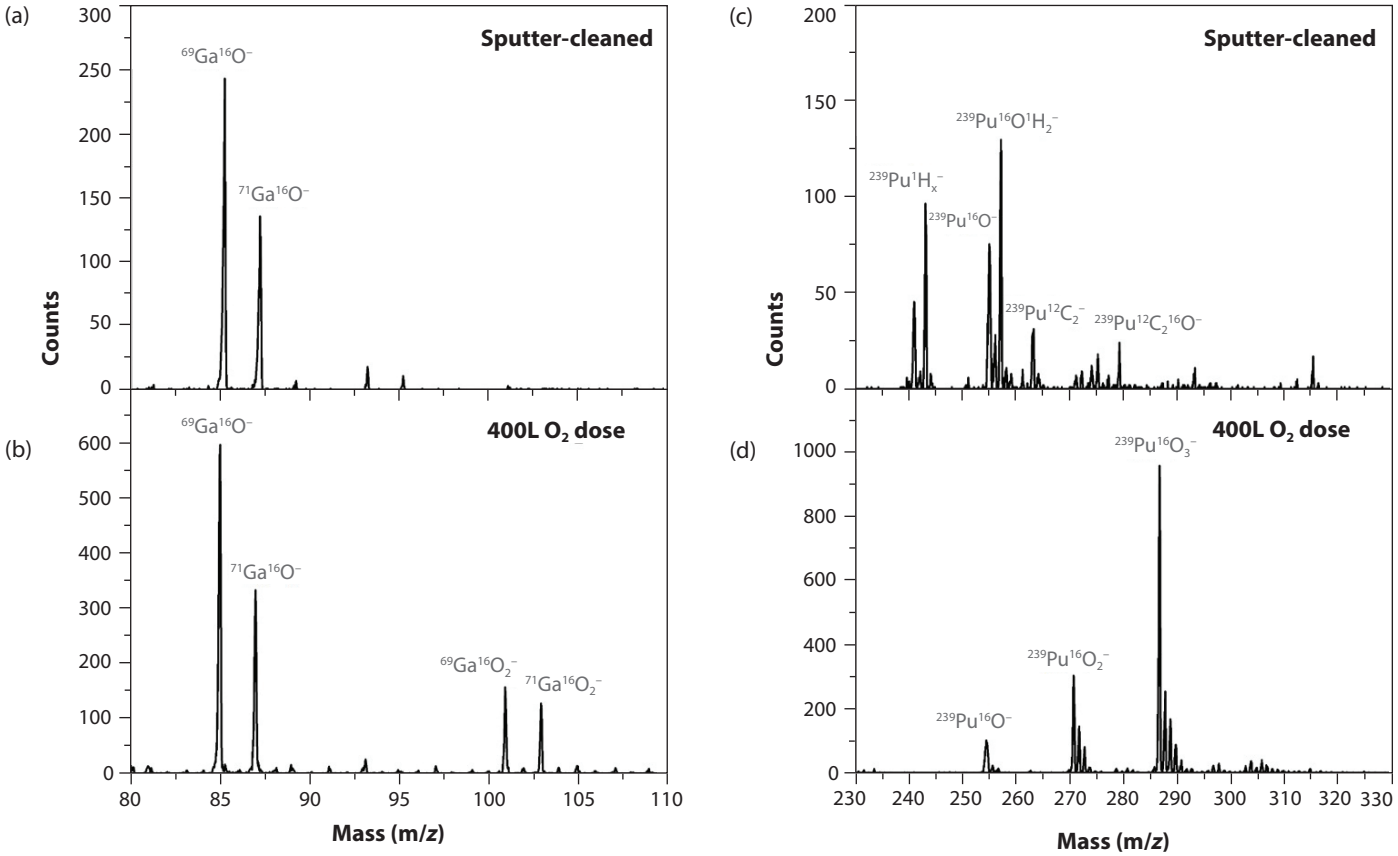

Figure 3. ToF-SIMS spectra for: **(a)** masses 80–110 sputter-cleaned and **(b)** after 400 L $^{16}O_2$ exposure; **(c)** masses 230–330 sputter-cleaned and **(d)** after 400 L $^{16}O_2$ exposure.

can deduce which fragments are from the material versus the gas phase. Sometimes this is not always intuitive, because scrambling of the fragments can occur and make analysis of the spectrum even more difficult.

One longstanding question concerns the reactivity of the alloying element Ga in stabilized δ-Pu that may exist on the surface, which could complicate the overall reactivity of this alloy. The δ-phase is the high temperature phase of Pu that has a face-centered cubic crystal system and shows favorable mechanical properties—Ga is used in small amounts (few atomic percent) to stabilize this phase at room temperature. ToF-SIMS has shown promise for elucidating the reactivity properties of Ga on the surface of δ-Pu, as described below.

Reactivity of gallium

The sample used in this experiment was a mechanically-polished 7 atomic percent (at. %) Ga-stabilized δ-Pu coupon (Fig. 2). In order to observe whether Ga is reactive on the surface, a 400 Langmuir (1 Langmuir, L = 10^{-6} Torr·sec) oxygen gas dose was applied to the surface. This is an equivalent of 400 atomic layers of $^{16}O_2$ on the surface. First, the sample was sputter-cleaned for approximately two minutes to remove surface containments and obtain the most pure metal possible (decreasing the yield of the secondary ions), and then exposed to 400 L of $^{16}O_2$. The ToF-SIMS instrument was a Kore Analytical system with a base pressure of 5×10^{-10} Torr.

After sputter-cleaning the sample, we observed peaks in the spectra at masses 85 and 87 (m/*z* values, where mass, m, is measured in Daltons, and charge, *z*, is the integral Coulombic charge, given as 1 in all the charged fragments considered here), corresponding to $^{69}Ga^{16}O^-$ and $^{71}Ga^{16}O^-$, respectively (Fig. 3a). Although the LMIG is a monoisotopic $^{69}Ga^+$ source and peaks associated with that particular isotope of

Acknowledgments

This work was supported by a Glenn T. Seaborg Institute Postdoctoral Fellowship and LANL Office of Experimental Sciences (C1). The author would like to thank her postdoctoral mentor, Thomas J. Venhaus, for guidance, teaching a "theorist" a new experimental technique, and his contributions to this work, and to the many people who helped from sample selection, preparation, and to installation of the Pu sample into the ToF-SIMS: Ron Allen, Ed Cagle, Claudette Chavez, Susie Duncan, John Dunwoody, James Gallegos, Paul Martinez, Jeremy Mitchell, Alison Pugmire, Mike Ramos, Scott Richmond, Joe Romero, Nyana Sanchez, Rachel Sanchez, Mike Torrez, Anthony Valdez, Darrell Vigil, and Kenneth Vigil.

Further reading:

1. *Flores, H.G.G., et al., Characterization and stability of thin oxide films on plutonium surfaces. Surface Science, 2011. 605(3–4): p. 314-320.*
2. *Flores, H.G.G. and Pugmire, D.L., The growth and evolution of thin oxide films on δ-plutonium surfaces. IOP Conference Series: Materials Science and Engineering, 2010. 9(1): p. 012038.*
3. *Morrall, P., et al., ToF-SIMS characterization of uranium hydride. Philosophical Magazine Letters, 2007. 87(8): p. 541-547.*
4. *Richmond, S., et al., The solubility of hydrogen and deuterium in alloyed, unalloyed and impure plutonium metal, IOP Conference Series: Materials Science and Engineering, 2010.*

Ga could be affected by the LMIG, the Pu sample has both Ga isotopes and, thus, fragments containing ^{71}Ga are best used to characterize the presence of the alloying agent within the Pu sample (natural isotopic ratio of ^{69}Ga:^{71}Ga is 60:40). The existence of these Ga-containing fragments indicates that Ga is located on the topmost surface and should not be ignored in surface reactivity studies.

In the Pu-containing high mass negative secondary ions (Fig. 3c), masses 240–243 appear, for which the simplest and most obvious assumption is that these ions are comprised of Pu and H atoms ($^{239}PuH^-$, $^{239}PuH_2^-$, $^{239}PuH_3^-$, $^{239}PuH_4^-$). If correct, the prominent peaks in the series would be associated with PuH_2^- and PuH_4^-. These peaks could be associated with small hydride spots on the sample as has been shown in previous work in the literature on uranium hydride. It is worth noting that the Pu sample studied in this work was not hydrided, as the sample was not exposed to H_2 gas, but laboratory air, and the oxide layer formed as a consequence (laboratory air implies that the air is composed of O_2, N_2, H_2O, etc.). As hydrogen is present in the Pu metal bulk phase at the atomic percent level, the existence of hydrides in the material will accelerate corrosion when H-containing gases (H_2O for instance) are present. As shown in Fig. 3c, there is also an increased intensity of the $^{239}Pu^{16}OH_2^-$ ($m/z = 257$) secondary ion peak with respect to the $^{239}Pu^{16}O^-$ fragment. A similar peak with U was also observed by Morrall et al., and therefore this suggests some correlation between the Pu-H series and the hydroxyl ($^{239}Pu^{16}OH^-$, $m/z = 256$) and hydrate peak ($^{239}Pu^{16}OH_2^-$). There are also Pu-C negative secondary ion fragments located at masses 263 and 279. Plutonium has an affinity to react with lighter elements such as carbon, oxygen, and fluorine, therefore the presence of carbon is inevitable if the sample has not been kept under a rigorously inert atmosphere.

After the 400 L $^{16}O_2$ gas exposure, peaks emerge at masses 101 and 103, which correspond to $^{69}Ga^{16}O_2^-$ and $^{71}Ga^{16}O_2^-$, respectively (Fig. 3b). This indicates that the surface Ga is reactive to gas dosing. Furthermore, the $^{239}PuH_x^-$ peaks have completely disappeared (after reaction with O_2) and only peaks containing Pu and O atoms remain. This implies that the $^{239}PuH_x^-$ peaks are only associated with the bare metal and not the oxide phase. We note that the $^{239}PuH_x^-$ peaks reappear when the oxide layer is removed via sputtering. The relative intensities of the PuO_x^- peaks are in the following order (Fig. 3d): $^{239}Pu^{16}O^-$ ($m/z = 255$) < $^{239}Pu^{16}O_2^-$ (271) < $^{239}Pu^{16}O_3^-$ (287). In comparison, the sample after sputter-cleaning (Fig. 3c) does not have a peak at 287 and has an extremely low intensity peak at 271. Therefore, the oxide layer formed after 400 L $^{16}O_2$ is different from the surface after sputter-cleaning, and the GaO_2^- fragments are found to be associated with the PuO_3^- fragment, implying that these ions are from the same oxide phase. The difference in oxide phase can only be determined by the relative intensity of the masses from ToF-SIMS; XPS would be more suitable in determining valence states as to whether it is a 4+ or 3+ state.

Summary and future work

ToF-SIMS can detect negative and positive secondary ion fragments, which gives us insight into the surface species that might exist. Our results reveal that Ga is located at the surface of Ga-stabilized δ-Pu and is reactive to O_2 exposure. We have shown that Ga is reactive to other environmental gas exposures also, such as water vapor (H_2O). Further studies are needed to fully understand the PuH_x fragments, and there are future plans to investigate a deuterium-loaded Ga-stabilized δ-Pu sample in order to determine the source of the hydrogen. As a whole, the suite of experimental surface science instruments within the PuSSL delivers a powerful ability to explore the oxidation and corrosion of Pu surfaces from a multitude of perspectives.

Actinide Research Quarterly is published by Los Alamos National Laboratory and is a publication of the Glenn T. Seaborg Institute for Transactinium Science, a part of the National Security Education Center. ARQ (est. 1994) highlights research in actinide science in such areas as process chemistry, metallurgy, surface and separation sciences, atomic and molecular sciences, actinide ceramics and nuclear fuels, characterization, spectroscopy, analysis, and manufacturing technologies.

LA-UR-19-20327

Address correspondence to:
Actinide Research Quarterly
c/o Editor
Mail Stop T-001
Los Alamos National Laboratory
Los Alamos, NM 87545

ARQ can be read online at:
www.lanl.gov/arq

If you have questions, comments, suggestions, or contributions, please contact the ARQ staff at:
arq@lanl.gov

National Security Education Center
David L. Clark, Director

G. T. Seaborg Institute for Transactinium Science
Science Advisors
Franz Freibert, Director (Acting)
Ping Yang, Deputy Director (Acting)

Editor
Owen Summerscales

Contributing editors
Susan Ramsay

Designers/Illustrators
Don Montoya
Owen Summerscales

Circulation Manager
Susan Ramsay


Los Alamos
NATIONAL LABORATORY
EST. 1943
NNSA
National Nuclear Security Administration